Quaternary International 430 (2017) 42–59

Contents lists available at ScienceDirect

Quaternary International

journal homepage: www.elsevier.com/locate/quaint

Elemental fingerprinting of Kenya Rift Valley ochre deposits for provenance studies of rock art and archaeological pigments

Andrew M. Zipkin [a, b, *], Stanley H. Ambrose [a], John M. Hanchar [c], Philip M. Piccoli [d], Alison S. Brooks [b, e], Elizabeth Y. Anthony [f]

[a] Department of Anthropology, University of Illinois at Urbana-Champaign, Urbana, IL 61801, USA
[b] Center for the Advanced Study of Human Paleobiology, The George Washington University, Washington, DC 20052, USA
[c] Department of Earth Sciences, Memorial University of Newfoundland, St. John's, NL A1B3X5, Canada
[d] Department of Geology, University of Maryland at College Park, College Park, MD 20742, USA
[e] Human Origins Program, National Museum of Natural History, Smithsonian Institution, Washington, DC 20560, USA
[f] Department of Geological Sciences, University of Texas at El Paso, El Paso, TX 79968, USA

ARTICLE INFO

Article history:
Available online 19 September 2016

Keywords:
Kenya Rift Valley
Ochre
Provenance
Provenience
LA-ICPMS
Central Kenya Peralkaline Province

ABSTRACT

The Kenya Rift Valley contains many ochre sources that are currently used by indigenous peoples for adornment, rituals, and art. Ochre pigments occur in rock art and archaeological sites spanning over 250,000 years. Chemical analysis for provenience of geological sources is the first step in the process of reconstructing provenance of archaeological artifacts for cultural heritage, archaeological, and paleoanthropological research. Development of an ochre source chemical composition database can facilitate reconstruction of social interaction networks and cultural heritage conservation efforts in this region. Techniques such as Laser Ablation-Inductively Coupled Plasma Mass Spectrometry (LA-ICPMS) and Instrumental Neutron Activation Analysis (INAA) are often used for compositional analysis and sourcing of ferruginous mineral pigments. Sourcing has proven challenging due to the diverse range of rocks and minerals that are classified as red and yellow ochres, and the diverse processes that induce variation in composition, including modes of formation, sedimentary transport of parent materials, and diagenesis. Attribution of samples to specific sources is possible only when variation within sources is less than differences between sources (the Provenience Postulate). Here we present the results of a study using LA-ICPMS to determine inter- and intra-source geochemical variations for ten ochre sources associated with three large volcanic centers in the central Rift Valley of Kenya. Our results show that differences in chemical composition among sources are greater than variation within sources, both at the scale of large volcanic centers and of individual ochre outcrops within these centers. Clear differentiation of source chemical fingerprints at local and regional scales satisfies the Provenience Postulate, and suggests that provenance studies of ochre artifacts, residues, and rock art in Kenya will be feasible.

1. Introduction

1.1. Overview of the study

Ochre is a term that encompasses a wide range of iron oxide minerals and iron oxide-rich rocks, clays, and soils that produce a colored streak. The use of red and yellow ochre pigments for symbolic purposes is a widespread and persistent human behavior (Wreschner et al., 1980). The creation of visual art and imagery to communicate information such as identities, symbols, signs, concepts, events, rituals, environmental features, and narratives is also an essential and enduring human attribute (Conkey et al., 1997; Nowell, 2006; Ross and Davidson, 2006; Ouzman, 2010; Fiore, 2014). While much of the human behavioral repertoire imbued with meaning is ephemeral (e.g. spoken language, dance), material symbols produced with mineral pigments are archaeologically persistent. The evidence for ochre use, symbolic and otherwise, extends back in time to greater than 250,000 years (Watts, 1999, 2009, 2014; McBrearty and Brooks, 2000; Barham, 2002; Deino and McBrearty, 2002; Hovers et al., 2003; Marean et al., 2007; Henshilwood et al., 2011; Burdukiewicz, 2014; Brooks et al., 2016).

In this study we test whether it is possible to distinguish among geologic deposits of ochre in the central and southern Kenya Rift

* Corresponding author. Department of Anthropology, University of Illinois at Urbana-Champaign, Urbana, IL 61801, USA
E-mail address: amzipkin@illinois.edu (A.M. Zipkin).

http://dx.doi.org/10.1016/j.quaint.2016.08.032
1040-6182/

Valley (KRV) of East Africa using Laser Ablation – Inductively Coupled Plasma Mass Spectrometry (LA-ICPMS). We undertook this pilot study in part because the diversity of geological contexts and formation processes represented in this region seemed likely to yield chemically distinctive ochres suitable for upholding the Provenience Postulate (Weigand et al., 1977) by elemental characterization, thus providing a basis for future sourcing studies of prehistoric and historic ochre artifacts and rock art pigments. The second rationale for this study is that the use of ochre in Kenya extends back in time to the Middle Stone Age (MSA) and continues to the present among Maasai and Samburu pastoralists, as well as other East African peoples (Section 2.2). This provides an opportunity for the ethnographic study of modern ochre source exploitation practices that are anthropologically significant in their own right, and may provide insight into prehistoric source selection criteria. In this pilot study we demonstrate that the Provenience Postulate (PP), which states that variation in composition within sources is less than differences among sources (Weigand et al., 1977), can be upheld for the ochre sources that we have analyzed in the Kenya Rift Valley. These results indicate the feasibility of additional ochre source survey and characterization in order to construct a more comprehensive database of source elemental "fingerprints" for provenience of archaeological ochre pigments and rock art in Kenya.

1.2. Provenience versus provenance: conceptual distinctions

Weigand et al. (1977) use the term provenience in their original definition of the Provenience Postulate, which only applied to chemical composition. Use of the term provenance is increasing, and is widely considered synonymous with provenience (Hirst, 2006). However, Joyce (2012, 2013) has thoroughly explicated important conceptual differences of these terms, as we will discuss below. Neff (2000) updated the PP to apply its principals to mineralogical composition and even qualitative characteristics, but substituted provenance for provenience because of the latter term's nearly universal use by archaeologists to refer to the location of discovery for an artifact (its archaeological context). Wilson and Pollard (2001) listed six assumptions and conditions that must be met as prerequisites for a geological/geochemical sourcing study, including Weigand et al.'s (1977) basic premise. The general theme of these definitions is an emphasis on the geographic location of a geologic material before it enters the archaeological record. This is analogous to the use of the term provenience by archaeologists to refer to the location of an artifact or feature within an archaeological site or on the landscape; both uses of provenience are limited to spatial considerations.

Pollard et al. (2014) reiterate the six conditions for satisfying the PP. They also expanded the scope of the versions of the PP described above, which they refer to as Traditional Provenance (but should be termed provenience as originally defined by Weigand et al., 1977), by considering the chronological dimension. Time is an important component of the anthropologically interesting dimension of artifact materiality inherent in the concept of object biography proposed by Gosden and Marshall (1999). This expanded definition aligns the concept of provenance more closely with its usage in art history and allied disciplines. It has been claimed that traditional provenance studies in archaeology treat transport as an instantaneous phenomenon without sufficient consideration of what happens between the place of raw material formation and the place of discovery of an object made from that material (Joyce, 2012, 2013; Pollard et al., 2014). This is not entirely accurate as even some early studies, such as Renfrew et al. (1966) on the prehistoric obsidian trade in the Near East, devoted considerable thought to modes of trade and transport. Joyce (2012, 2013) thoroughly discusses the conceptual distinction of provenience as geological location versus provenance as object biography, following conventional usage in the field of art history. Joyce's concept of provenance encompasses all aspects of the history of human interaction with an object including raw material acquisition, transport, modification, transfer of ownership (chain of custody), functions, and symbolic meanings.

Our survey of the geological literature shows that the term provenience is rarely used, and provenance is used mainly in sedimentary geology, where it refers to the origin *and* transport history of sedimentary particles from bedrock source to sedimentary deposition site (Haughton et al., 1991; Weltje and von Eynatten, 2004). Geologists' use of provenance is thus conceptually allied with that of art historians and archaeologists investigating object and place biographies. A summary of the results of a poll on usage of these terms in archaeology (Hirst, 2006) concludes with this apt analogy: "Provenience is an artifact's birthplace, while Provenance is an artifact's resume". However, as previously noted, archaeologists also use the term provenience for the spatial location of an object within an archaeological site (its deathplace).

Throughout this paper we will use provenience in this spatial sense to refer to both the location of geological sources of ochre, and the location of ochre pigments in archaeological and rock art sites (archaeological provenience). In contrast, our use of provenance includes all processes that a characterized material is subjected to by humans during its life history, beginning with its geological provenience and ending with its archaeological provenience. We also propose adding post-depositional processes (taphonomy, chemical diagenesis) to the life history concept of provenance. In the case of rock art, provenience analysis of pigments can be an important component of reconstructing place biographies: sites that have developed histories of use through the application of pigments from different sources over time. Fulfilling the requirements of the PP by discriminating among geologic sources is the essential first step in the anthropological archaeological investigation of provenance of objects, places, and people.

1.3. Ochre composition analysis

The single greatest analytical challenge for ochre provenience and provenance studies is that ochre is not a single type of rock or mineral (Popelka-Filcoff et al., 2008). Although other naturally occurring red streaking pigments are well known to archaeologists, for example, cinnabar (HgS), they are considered distinct from ochre because they are not colored by iron minerals (e.g., Mioč et al., 2004). Ochreous rocks, clays, and soils may derive their color from chromophore minerals such as hematite (α-Fe_2O_3), goethite (α-FeOOH), ferrihydrite ($Fe_5O_8H \cdot H_2O$), lepidocrocite (γ-FeOOH) (Cornell and Schwertmann, 2003), and jarosite ($KFe_3[SO_4]_2(OH)_6$) (Jercher et al., 1998), to name a few well-known examples. No more than 1–1.5% iron is required to color a lateritic soil red or orange (Cornell and Schwertmann, 2003) and render it suitable for use as a pigment. These chromophore minerals may also be considered ochre in their own right when they occur independently or as the primary constituent of a rock, such as hydrothermal vein hematite or an iron oxide-rich gossan formed by the surface weathering of an Fe-rich ore body exposure. Due to the diversity of materials involved there is no single best approach to a provenience study of ochre. Rather, the choice of analytical method needs to be tailored to the variables that are most likely to uphold the PP while simultaneously minimizing damage to the cultural materials of interest. Thus, the optimal method for a given study is whichever technique facilitates the measurement of variables that exhibit high intra-source homogeneity and high inter-source heterogeneity.

Geochemical characterization and sourcing studies of ochre have used techniques such as LA-ICPMS (Green and Watling, 2007; Eerkens et al., 2012; Bu et al., 2013; Zipkin et al., 2015), solution

Multi Collector-Inductively Coupled Plasma Mass Spectrometry (MC-ICPMS) (Eerkens et al., 2014), Inductively Coupled Plasma-Optical Emission Spectrometry (ICP-OES) (Dayet et al., 2015; Moyo et al., 2016), Instrumental Neutron Activation Analysis (INAA) (Popelka-Filcoff et al., 2007, 2008; Eiselt et al., 2011; MacDonald et al., 2013), Attenuated Total Reflectance Fourier-Transform Infrared Spectroscopy (ATRF-TIS) (Vahur et al., 2010), micro-Raman and micro-Fourier Transform Infrared Spectroscopy (FTIR) (Bikiaris et al., 1999), Thermogravimetric Analysis (TG), Differential Scanning Calorimetry (DSC), and Mass Spectrometry (Thomas et al., 2011), Scanning Electron Microscopy – Energy Dispersive X-ray Spectroscopy (SEM-EDS) (Huntley et al., 2011), Particle Induced X-Ray Emission (PIXE) (Mathis et al., 2014), and powder X-Ray Diffraction (XRD) (Matarrese et al., 2011; Dayet et al., 2013; Huntley et al., 2014; Cavallo et al., 2015). Research using a suite of multiple archaeometric techniques to analyze mineral pigments is becoming increasingly common (e.g. Dayet et al., 2015; Chalmin et al., 2016; Moyo et al., 2016). Such studies, coupled with technical advances and basic research on chronometric dating of rock art paints (e.g. Sauvet et al., 2015a and subsequent commentary: Pons-Branchu et al., 2015; Sauvet et al., 2015b; Aubert, 2016), may foreshadow the emergence of a standard toolbox of inter-dependent methods for investigating archaeological coloring materials.

The significance of adapting powerful geochemical techniques such as LA-ICPMS and MC-ICPMS for characterizing and distinguishing among geologic sources of ochre is twofold. First, a reliable, minimally destructive method for sourcing ochres will allow researchers to study mineral pigments from a landscape perspective with an emphasis on source exploitation patterns, transport distances, and detecting trade networks, with implications for social and territorial organization. This quantitative microanalytical approach to source provenience is applicable to ochre artifacts and residues, as well as to rock art sites painted with ochre pigments. Microanalysis thus contributes to the feasibility of provenance research on object and place biographies (Boivin, 2004; Pollard et al., 2014). Second, with regard to rock art in particular, pigment compositional analysis and provenance research has the potential to aid efforts to conserve rock art sites and detect recent modifications to them.

2. Ochre and human behavior

2.1. Symbolic and functional uses of ochre

Ethnographic records of ochre use, mainly in Australia, show that some ochre sources were strongly preferred for symbolic reasons, and were transported over long distances (Mulvaney, 1978; Peterson and Lampert, 1985; Taçon, 2008). Symbolic roles include use as a substrate for engraved designs (Mackay and Welz, 2008; Henshilwood et al., 2009), cosmetic (Thackeray et al., 1983; Saitoti, 1993; Watts, 2009; Simpson and Waweru, 2012), and pigment for portable and rock art (Chamberlain, 2006; Mulvaney, 2013; Scadding et al., 2015; Rifkin et al., 2016). Functional applications or perhaps dual symbolic-functional uses include hide preservative (Audouin and Plisson, 1982; Rifkin, 2011), food and wood preservative (Erlandson et al., 1999), internal medicine (Velo, 1984), sunscreen/skin protectant and wound plaster (Peile, 1997; Rifkin et al., 2015), birthing lubricant (Kamwendo, 2009), and an ingredient in composite tool hafting adhesives (Brandt and Weedman, 2002; Wadley et al., 2004; Lombard, 2005; Helwig et al., 2014; Zipkin et al., 2014; Kozowyk et al., 2016). Ethnographic studies of ochre source exploitation, transport and processing, and symbolic, aesthetic, and functional uses can help test alternative hypotheses about culturally mediated source exploitation versus least-cost energetics (closest source and gravity) null-models of source use in the archaeological record. Reconstructing patterns of ochre source use with geochemical methods could shed new light on the spatial transport and exchange of these mineral pigments, and thus the symbolic dimensions of ancient socially and culturally constructed landscapes.

2.2. Ethnographic, archaeological and rock art research on ochre use in East Africa

With a few notable exceptions, rock art in the Kenya Rift Valley is understudied relative to the rest of East Africa (Posnansky and Nelson, 1968; Chaplin, 1974; Odak, 1977; Masao, 1979; Leakey, 1983; Mabulla, 2005; Chamberlain, 2006; Russell, 2013). This is somewhat surprising in light of the fact that Maa-speaking Maasai and Samburu peoples of this region still regularly use ochre and other pigments for their active rock art traditions. For example, Gramly (1975a) identified 19th century through modern Maasai warrior's shield motifs executed in red ochre and black and white pigments at the Leshuta rock shelter (GwJg2) meat feasting site in southwest Kenya (Fig. 1). This site and nearby caves and rock shelters (GwJg14, at the same location on Fig. 1 as GwJg2) were revisited in 2006 and 2008 by Ambrose, and in 2015 by Ambrose, Zipkin, Mercy Gakii and David Coulson for detailed study, and they show continued use for meat feasting and painting. Gramly (1975a, 1975b) also documented numerous painted rock shelters at Lukenya Hill. Subsequent surveys of rock art at Lukenya Hill from 1975 to 1980 (C.M. Nelson and J. Swan, field notes and site registry forms on file at the National Museums of Kenya) have substantially increased the number of painted sites, and a significant case of rock art forgery and overpainting of a Maasai and pre-Maasai rock art panel was discovered in 1995 (Ambrose, 2007). Rock paintings occur throughout Maasai and Samburu territories (Chamberlain, 2006; Coulson, 2006; Russell, 2013), and some localities continue to be painted to this day. Most rock art sites remain extremely poorly studied. Moreover, ethnographies are virtually mute on the meanings of paintings and the uses of ochre (Chamberlain, 2006).

In addition to recently created and likely ancient rock art, Kenya has many archaeological sites containing ochre artifacts and residues. The oldest examples are Middle Pleistocene in age, including the >5 kg of red ochre reported by Deino and McBrearty (2002) from the Kapthurin Formation, Baringo, Kenya (>284 ka) and two ochre artifacts, one partially perforated, from Olorgesailie, Kenya which date to at least 220 ka and possibly to older than 300 ka (Brooks et al., 2016). In a notable younger example, at Enkapune Ya Muto rockshelter (GtJi12) ochre residues are preserved on a grindstone and on two flakes from the basal layer, which contains the Middle Stone Age (MSA) to Later Stone Age (LSA) transitional Endingi Industry (>50 ka), on several backed blades from the earliest LSA Nasampolai industry (>40 ka) in locations that indicate ochre was a component of hafting adhesive, and on ostrich eggshell artifacts from the early LSA Sakutiek industry (35–40 ka) (Ambrose, 1998). At Njoro River Cave, an Elmenteitan Neolithic burial site, approximately 80 burials were interstratified with layers of red ochre, including a basal layer up to several inches thick. Many ochre-stained upper grindstones (pestle-rubbers) were recovered (Leakey and Leakey, 1950), and 45 of 77 lower grindstones were ochre-stained (Robertshaw and Collett, 1983). Pottery with red slip, large chunks of ochre, and ochre-stained grindstones are common in some sites of the Kansyore tradition in the eastern Lake Victoria Basin (Dale and Ashley, 2010).

Red ochre continues to be used in traditional settings among Maa-speaking pastoralists and has been documented for other Kenyan peoples such as the Kikuyu (Lawren, 1968) and the Okiek (Blackburn, 1971). For example, Maasai and Samburu warriors and women use red ochre for coloring ornaments, house walls, clothing, hair, and skin. However, detailed ethnographic studies of *how* ochre

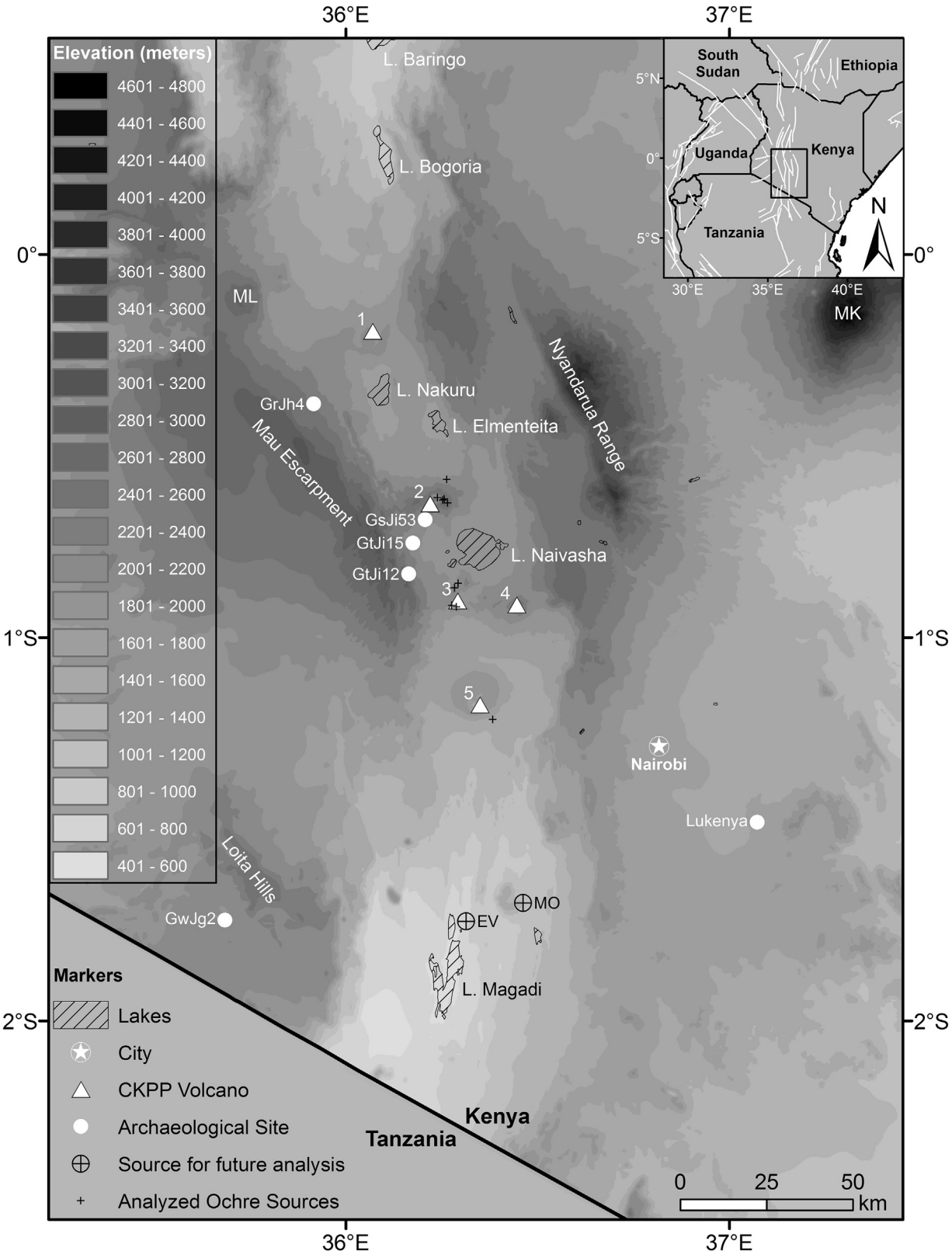

Fig. 1. Overview of the Central Kenya Peralkaline Province (CKPP) study area within the Kenya Rift Valley. The 250 m resolution Digital Elevation Model was created by the International Livestock Research Institute and the Japan International Cooperation Agency, derived from the Survey of Kenya 1:250,000 Topographic Map (1996). Centers of volcanic activity in the CKPP during the Holocene (Smithsonian Global Volcanism Database version 4.3.3) are indicated by Δ: 1 – Mount Menengai, 2 – Eburru Volcanic Complex (EVC), 3 – Greater Olkaria Volcanic Complex (GOVC), 4 – Mount Longonot, 5 – Mount Suswa. Additional mountains labeled as landmarks include MK: Mount Kenya and ML: Mount Londiani. Some ochre-containing archaeological sites are indicated by open circles (○): Njoro River Cave (GrJh4), Oltepesi Rockshelter (GsJi53), Marmonet Drift (GtJi15), Enkapune Ya Muto (GtJi12), Leshuta Rockshelter and Caves (GwJg2 labeled, GwJg14 is at the same location), Lukenya Hill (GvJm16 and other sites reported by Gramly, 1975b). Sources of ochre that will be analyzed in future research are indicated by ⊕: MO: Mount Olorgesailie, EV: Enjompolei Valley. Ochre sources sampled and analyzed for this study are indicated by +. The inset map shows the study area (rectangle) in regional context. White lines indicate the faults and tectonic contacts of the East African Rift System.

is used, and especially how it is acquired and processed, are lacking. These gaps in the ethnographic record are remarkable considering the fact that ochre is still widely used at present. In a rare exception, Nakamura (2005) provides a thorough and systematic description of Samburu ochre use, including ritual marking of important stages of life with large amounts of ochre, notably the achievement of warrior status and female circumcision. Nakamura (2005) noted that some ochre is purchased in markets, so its primary sources remain undocumented. Chamberlain (2006: 143) stated that on several occasions Samburu informants "…commented that they could identify the age-set that had drawn the [rock art] motifs through the type of red ochre that had been used, as each age-set has a shade and consistency unique to them." However, her informants did not identify ochre proveniences. Many Maasai and Samburu individuals know the locations of traditionally used ochre sources. For example, during fieldwork in 2012 Maasai and Samburu informants guided two of the authors to seven previously undocumented ochre outcrops in the KRV, and to an additional 41 sources in 2015 and 10 sources in 2016 that were used by these individuals.

2.3. Provenience analysis and heritage management

The widespread presence of ochre at prehistoric and modern cultural sites in East Africa underscores the importance of refining methods for mineral pigment composition analysis, identifying geologic deposits of ochre, and characterizing the elemental fingerprints of those sources to facilitate geologic provenience, and broader provenance, research in the region. In addition to the implications for investigating transport of mineral pigments for reconstructing trade, social exchange, mobility and resource exploitation patterns, the ability to reliably provenance ochre used in rock art is relevant to the preservation of such sites. One of the first studies to apply LA-ICPMS to ochre provenience was undertaken to identify stolen or forged Australian Aboriginal artwork (Green and Watling, 2007). The need to detect forged or recently modified rock art is no less important in Kenya. For example, at Lukenya Hill rock art site GvJm16 (labeled Lukenya on Fig. 1), recent additions to and overpainting of the main wall of Maasai and pre-Maasai paintings included images of a giraffe, and a human in a trance-like pose in styles characteristic of the Kondoa regions of central Tanzania (Leakey, 1983), which has potential links to the rock art of southern Africa (Lewis-Williams, 1987). Investigations in collaboration with David Coulson of the Trust for African Rock Art (TARA) (Ambrose, 2007) revealed that the site was overpainted during the production of the *Young Indiana Jones* television series (episode 2, "Passion for Life"). If this forgery had not been recognized on the basis of before-and-after photographs and Gramly's tracings of the painted images at this site, it could have severely distorted our understanding of the geographic distribution of this rock art tradition, and the past distribution of Khoisan speakers. The Lukenya Hill case is an exceptional example of the damage that can be done to a rock art site, as well as the potential for making erroneous revisions of cultural history, that can prevented by identifying recently modified rock art. Refining methods to provenience pigments, and for dating rock art (David et al., 2013), can provide powerful new tools for cultural heritage research and preservation.

3. Geologic context of the study area

3.1. The Central Kenya Peralkaline Province

The KRV (Fig. 1, inset map) is an active continental divergence zone within the greater East African Rift System. It runs from northeast of Lake Turkana in southern Ethiopia through Kenya and into the Lake Natron basin of northern Tanzania with a depth of approximately 1 km and an average width of 60–80 km (Darling et al., 1995). The earliest volcanism in the East African Rift System is documented in the northern Turkana depression around 45 Ma, with the earliest extension of the rift in this area beginning around 25 Ma (Furman, 2007). This region is characterized by a high geothermal gradient due to the shallow depth of the Mohorovičić discontinuity, which ranges from 20 km in northern Kenya, and 35 km beneath the Kenya Dome, to 38 km in northern Tanzania (Keller et al., 1994; Lagat, 2003; Ren et al., 2006). Although all volcanoes in the KRV are dormant except for Ol Doinyo Lengai in northern Tanzania, which erupted as recently as 2013 (Global Volcanism Program, 2013), many possess convective geothermal systems that manifest at the surface as fumaroles, hot springs, and hydrothermally altered sediments (Darling et al., 1995; Biggs et al., 2009). During several obsidian source and archaeological site surveys in the KRV undertaken prior to this study (Bower et al., 1977; Ambrose, 1984; Merrick and Brown, 1984; Coleman et al., 2008), numerous occurrences of fumaroles with associated ochre in the vicinity of Mt. Eburru and the Olkaria volcanic complex were observed. Similar fumaroles where hematite and goethite encrustations co-occur with clay minerals such as kaolinite ($Al_2Si_2O_5[OH]_4$), smectite group clays such as montmorillonite ($[Na,Ca]_{0.33}[Al,Mg]_2[Si_4O_{10}][OH]_2 \cdot nH_2O$), and illite ($K_{0.6–0.85}[Al,Mg]_2[Si,Al]_4O_{10}[OH]_2$) have been noted elsewhere, for example in the Valley of Ten Thousand Smokes, Alaska (Keith, 1991).

The area of interest for this project (Fig. 1) is the Central Kenya Peralkaline Province (CKPP), a ~6000 km^2 region within the KRV characterized by five relatively young volcanic centers with peralkaline (i.e., igneous rocks with an excess of $[Na_2O + K_2O]/Al_2O_3$) compositions (Scaillet and MacDonald, 2003; MacDonald and Scaillet, 2006; MacDonald and Bagiński, 2009). The KRV bisects the crustal uplift of the Kenyan Dome and the location of the CKPP corresponds to the apex of this uplift (Baker et al., 1988; MacDonald and Scaillet, 2006; White et al., 2012a; White et al., 2012b). The five volcanic centers of the CKPP, the rhyolitic dome complexes of Eburru and Olkaria, and the trachytic caldera volcanoes Menengai, Longonot, and Suswa, show distinct eruptive products despite their relatively close geographic proximity to one another (Lagat, 2003; MacDonald and Scaillet, 2006; White et al., 2012a; White et al., 2012b). MacDonald and Scaillet (2006) attribute this to separate magmatic systems supplying the eruptive products for each complex; partially molten high-level reservoirs for the complexes may be present at <10 km depth. The geochemical distinctiveness of each volcano complex in the CKPP made this a particularly suitable area for our investigation of the feasibility of using elemental fingerprints to discriminate among ochre sources. Samples (Fig. 2) were collected from ochre sources within the Eburru Volcanic Complex (Fig. 1, Volcano #2), the Greater Olkaria Volcanic Complex (Fig. 1, Volcano #3), and the Suswa shield volcano (Fig. 1, Volcano #5) during August of 2012.

For the purposes of this study, the most important general distinction between the three volcanic centers is whether their peralkaline eruptive products are classified as comenditic or pantelleritic. MacDonald (1974) divided peralkaline extrusive rocks into four groups based on whether they are rhyolitic (silica-enriched) or trachytic (relatively low Si) and on their total Al_2O_3 and FeO content: comenditic trachyte (high Al, variable Fe), pantelleritic trachyte (variable Al, high Fe), comendite (variable Al, low Fe), and pantellerite (low Al, variable Fe). Higher iron content volcanic parent rocks are more likely to yield weathering products containing sufficient amounts of iron chromophore minerals such as hematite (red) or goethite (yellow) for use as pigment. Although, as noted previously, only 1% Fe content can have a dramatic effect on color, higher iron oxide content and lower amounts of accessory minerals generally yield higher quality ochre pigment. In a study of

Fig. 2. Photographs of some ochre sources sampled during the 2012 field season and analyzed for this project. a. Eburru Steam Condenser 1 source sampling area with active fumaroles. b. Moshi ya Maji ochre source sampling location in an active fumarole adjacent to an obsidian quarry site, also within the Eburru Volcanic Complex. c. Olkaria Gate ochre source near entrance to Hell's Gate National Park. The inset shows an ochre sampling location where one of the authors is standing in the larger image. d. Suswa Southeast Slope, Locality 1 ochre source with sampling location indicated by Maasai guides, underlying a welded tuff or lava flow. All four sources have evidence of hydrogeothermal activity.

the behavior of iron during the weathering of rhyolites from Kozushima Island, Japan, Yokoyama and Nakashima (2005) observed that as weathering progresses iron is dissolved from the parent rock and precipitates as ferrihydrite, which eventually alters to goethite. This corresponds with increasing yellow and redness of the alteration products as weathering progresses. Schwertmann and Cornell (1991, p. 58) note that elevated temperature favors the formation of hematite over goethite from ferrihydrite; this suggests that surface manifestations of geothermal activity in the CKPP will be associated with red ochre deposits formed from the weathering of iron-rich volcanic rocks.

3.2. Eburru Volcanic Complex (EVC, 0.65°S, 36.22°E)

The EVC, located northwest of Lake Naivasha, covers approximately 470 km^2 of the Rift Valley and is made up of three geographic components: Western Eburru, Eastern Eburru, and Waterloo Ridge (Clarke et al., 1990). The volcanic rocks of the EVC can be broadly characterized as pantellerite and pantelleritic trachytes. Four stages of volcanic evolution have been defined for the complex, which formed from west to east (Clarke et al., 1990; Ren et al., 2006). Formation of the Eburru massif began with a volcanic pile in Western Eburru. The second phase of volcanism involved a succession of pyroclastic eruptions along a north-south aligned fissure zone east of the main massif. This resulted in the formation of the 19.5 km long Waterloo Ridge (Clarke et al., 1990; MacDonald and Scaillet, 2006). Stage three involved building a volcanic pile in Eastern Eburru, which is linked to Western Eburru by a saddle. Both Eastern and Western Eburru exhibit ring structures, though Western Eburru is difficult to map because of vegetation cover (Velador et al., 2002, 2003). Cumulatively, the massif formed by Western and Eastern Eburru comprises 92% of the area of the EVC, with the balance made up by the morphologically separate Waterloo Ridge (Clarke et al., 1990). At least 50 craters, as well as many domes, lava flows, and cones, are present today towards the eastern end of the massif (Clarke et al., 1990; Ren et al., 2006). The youngest eruptive products (stage four) are found in Eastern Eburru where obsidian flows are encountered along north-south running faults (Ren et al., 2006). Based on field observations and correlations with dated lava flows elsewhere in the Kenya Dome, most volcanic activity in the Eastern Eburru and Waterloo Ridge is no older than ~0.25 Ma.

Geothermal energy exploitation potential was assessed by the Kenya Electricity Generating Company (KenGen) (Allen et al., 1989). Remote sensing studies identified numerous fumaroles within the EVC, 80% of which are associated with north-south trending faults in Eastern Eburru (Velador et al., 2003). Kubai and Kandie (2014) confirmed the results of the earlier remote sensing survey; the distribution of fumaroles, hot springs, and thermally altered ground within the EVC is related to local and regional faults. Our survey and sampling of ochre sources emphasized Eastern Eburru where fumaroles are readily accessible (Fig. 2a, b). Velador et al. (2003) estimated that faulting in Eastern Eburru occurred between 0.8 and 0.4 Ma. If the onset of fumarolic activity and the formation of ochre deposits from fumarolic weathering of volcanic rocks

followed faulting then ochre sources in this area would have been available to MSA and more recent inhabitants for pigment exploitation. Ochre sources were identified in the Eastern Eburru Pantellerite Formation and the Eburru Pumice Formation. Eburru pantellerites generally range in whole rock FeO_{tot} (wt%) from ~6 to 9% (MacDonald and Scaillet, 2006), an ample amount of iron to yield high-quality ochre weathering products.

3.3. Greater Olkaria Volcanic Complex (GOVC, 0.90°S, 36.29°E)

Located immediately south of Lake Naivasha, and west of the Longonot stratovolcano, the GOVC spans roughly 240 km^2 with at least 80 recognized centers of volcanic activity (Clarke et al., 1990; Rogers et al., 2004). These eruptive centers formed short, thick lava flows and domes, of which the largest is Olkaria Hill, at 2 km basal diameter and 340 m height. Marshall et al. (2009) identified 13 geochemically and petrographically distinct centers that dominate eruptive activity in the GOVC. In addition to prominent individual domes like Olkaria Hill, the topography of the GOVC is comprised of coalesced domes and lava flows forming distinct groups of hills and ridges. The most prominent non-eruptive feature of the GOVC is Hell's Gate Gorge, from which the National Park encompassing much of the complex derives its name. Clarke et al. (1990) divide the gorge into a northern section referred to as Hell's Gate and southern section referred to by the Maasai name *Ol Njorowa*. The gorge bisects the GOVC from northeast to southwest, separating Olkaria Hill and the other western domes from an arc of domes east of the gorge. All of the GOVC ochre sources sampled in 2012 are located between Olkaria Hill and the gorge in areas identified by Clarke et al. (1990) as the Lower and Upper Members of the Olkaria Comendite Formation.

The lithology of the GOVC is composed of unconsolidated pyroclastic sediments overlying a volcanic sequence made up of rhyolite, trachyte, basalt, tuff, and doleritic and syenitic dykes (Lagat, 2007). In contrast to the largely pantelleritic trachytes and rhyolites of Eburru, Velador et al. (2002) note that the volcanic rocks exposed at the surface in the GOVC are generally comenditic (i.e., lower Fe content and higher Al content than pantellerite). The oldest Comendite lavas in Ol Njorowa Gorge are 322 ± 20 kyr (Trauth et al., 2003). The surface GOVC rocks are estimated to be <20,000 years old (Marshall et al., 2009). Clarke et al. (1990) reported a radiocarbon date of ~180 years B.P. on carbonized tree roots from a pumice flow, indicating that some areas of the GOVC have been active quite recently.

The Olkaria geothermal field is an important source of clean, renewable energy whose heat source is a shallow magma body identified in a seismic wave study by Omenda (2005). A 2012 KenGen report on the Olkaria IV Domes Geothermal Project noted that focus group interviews with local residents indicated that the Ol Njorowa Gorge area of the GOVC contains fumarole-associated deposits of red ochre and white clay pigments that are highly regarded by the Maasai people of Kenya. These deposits are of such importance that the entire complex, as well as the prominent landmark Olkaria Hill and a much smaller outcrop with evidence of past fumarolic activity located near the north entrance to the National Park (Fig. 2c), is named for one of the Maa words for red ochre: *ol-karia* (Mol, 1978).

Lagat (2007) described the metasomatism of minerals by hydrothermal fluids within the Olkaria geothermal field, and noted the formation of clay minerals from the alteration of feldspar and volcanic glass and of hematite from the alteration of olivine and magnetite present in the area's primary volcanic rocks. Preliminary mineralogical research reported by Clarke et al. (1990) identified halloysite ($Al_2Si_2O_5(OH)_4$), a disordered form of kaolinite, as the most common phase in hydrothermally altered rocks in the Lake Naivasha region, which includes the GOVC. Kaolinite, chlorite, and smectite are also present in some cases. Clarke et al. (1990) noted that while thermally altered rock ranged in color from cream-yellow to reddish-pink, some samples exhibited intense red coloration. Multiple deposits of red ochre associated with fumarolic activity were sampled during our survey of the GOVC.

3.4. Mt. Suswa Volcano (1.18°S, 36.35°E)

Located ~45 km south of Lake Naivasha and ~30 km south-southeast of our GOVC study area, Mount Suswa is a distinctive trachytic-phonolitic shield volcano with a spectacular double caldera composed of a ring graben within the older caldera that surrounds a tilted central island block (Randel and Johnson, 1991). The evolution of the volcano, which covers more than 700 km^2, has been divided into three major stages (Johnson, 1969; MacDonald et al., 1993; White et al., 2012a; White et al., 2012b; Guth and Wood, 2014). MacDonald and Scaillet (2006) date the beginning of volcanic activity, the pre-caldera stage of lava shield building, to <0.4 Ma. Based on U-series disequilibria dating, which show values of $^{230}Th/^{232}Th$ less than unity (U-series data provided in Table 1), we prefer the more precise age of <0.24 Ma. The characterization of pre-caldera Mt. Suswa as a low-angled shield volcano originated with Johnson (1969) but has been questioned in more recent publications (Skilling, 1993). The syn-caldera stage began with the collapse of the caldera roof; this was accompanied by low volume pyroclastic eruptions of carbonate-rich trachytes from an outer ring feeder zone. White et al. (2012b) reported preliminary dates of ~0.12 Ma for lavas in the main caldera wall. The post-caldera stage featured the partial filling of the original caldera with lava flows from 12 ka to recent and the subsequent formation of the 2356 m summit known as Ol Doinyo Nyukie (The Red Mountain) from porphyritic phonolite lavas (Johnson, 1969; White et al., 2012b; Guth and Wood, 2014). Following the eruption of the Ol Doinyo Nyukie lavas, withdrawal of magma formed a pit crater, partially collapsing the Ol Doinyo Nyukie cone, and eventually to a second collapse inside the original caldera, which created a spectacular ring graben with a central island block (Skilling, 1993; Wooley, 2001).

Table 1
Uranium (U) series isotopic data for Suswa volcano. Uranium decays via alpha and beta emissions to its stable daughter lead (Pb). For anthropologic and geologic studies, the most commonly measured intermediate daughter isotopes are ^{234}U and ^{230}Th. Concentration ratios of these daughters were calculated to either their parent (^{238}U) or to ^{232}Th, which has a very long half-life (~1.4 × 10^{10} years) and thus can be considered stable within the context of the intermediate daughters. Ratios other than unity represent disequilibrium in the U-series and indicate that the sample formed less than 250,000 years ago.

Sample no:	Suswa							
	KS/94/26	KS/94/29	KS/94/03	KS/94/39	KS/94/44	KS/94/01	KS/94/02	KS/94/49
U (p.p.m.)	4.98	7.56	2.94	6.55	4.57	4.82	4.86	6.14
Th (p.p.m.)	25.2	40	17.2	30.5	21.9	22.2	22.7	28.2
($^{234}U/^{238}U$)	1.000	0.999	1.000	1.001	1.000	1.000	0.998	1.002
($^{238}U/^{232}Th$)	0.604	0.578	0.523	0.656	0.637	0.663	0.655	0.655
($^{230}Th/^{232}Th$)	0.678	0.722	0.764	0.85	0.847	851	0.853	0.851
($^{230}Th/^{238}U$)	1.123	1.250	1.426	1.296	1.331	1.284	1.302	1.279

Surface manifestations of geothermal activity on Mt. Suswa were first reported by Spink (1945; Spink and Stevens, 1946; Randel and Johnson, 1991, p. 35), including ~25 steam jets and fumaroles in the vicinity of a small scoriaceous cone named Soit Amut: (also spelled Soit Amurt), which formed on the lower southern slopes of Suswa during the pre-caldera eruptive stage. McCall and Bristow (1965) also noted the presence of extensive fumarolic activity and associated metasomatically altered rocks including heavily kaolinized phonolites. More recent publications have emphasized that most of the fumarolic activity is not on the flanks of the volcano where it was originally noted by Spink (1945) but instead is found in the ring structures of the inner and outer caldera (Darling et al., 1995; Omenda, 2008; Simiyu, 2010). A conceptual model based on seismic, gravity, and gas thermometry studies suggests that the geothermal heat source for Suswa is a magma body beneath the inner and outer caldera and centered under Ol Doinyo Nyukie at a depth of 6–8 km (Omenda, 2008). More recent seismic and gravity studies by Simiyu (2010) indicate that the magma body beneath the caldera is deeper, at 8–12 km. Mount Suswa geothermal energy generation potential assessment by KenGen is limited to three exploratory wells that were sunk in 1999.

Mount Suswa received the least extensive ochre source survey coverage of the three study areas during the 2012 season. All samples were from two discrete outcrops identified by local Maasai informants, located 1.2 and 1.7 km north of Soit Amut. Samples from the southern locality analyzed for this project underlie a welded tuff or lava (Fig. 2d). Steam vents were also noted approximately 0.5 km away at the second locality, from which only one sample was collected and awaits analysis. It is clear that, based on the abundance of ochre outcrops associated with fumarolic activity in Olkaria and Eburu, intensive survey of the Suswa caldera is needed for comprehensive assessment of CRV ochre source chemical variation.

4. Materials and methods

4.1. Sample collection

Samples collected from ten ochre sources in Kajiado and Nakuru counties, Kenya, during the 2012 field season were analyzed for this study (Table 2). Additional ochre sources sampled in 2012 but not yet analyzed include Mount Olorgesailie and Enjompolei Valley (labeled on Fig. 1) and Mount Suswa locality 2 (0.5 km north of the source of analyzed samples indicated on Fig. 1). Some sources had previously been identified by Ambrose during obsidian source surveys while others were located with the assistance of local Maasai guides during the 2012 season. Multiple samples were collected from each source in order to gauge intra-source heterogeneity, with particular attention paid to collecting samples of each color of ochre present. We did not systematically seek guidance from our informants on sampling within sources. Our collection of ochre samples and record of source locations is not comprehensive. This study was undertaken as a preliminary investigation into the viability of distinguishing among volcanic center-associated ochre deposits by characterizing intra- and inter-source chemical variation. Testing the Provenience Postulate among the limited number of sources considered here will inform the direction of future research and the construction of a more comprehensive source database.

Table 2
Summary of sources sampled and analyzed in this study. Individual sample descriptions, coordinates, and geologic contexts are presented in Table S3.

Ochre source	Volcanic center (# on Fig. 1)	# of samples analyzed	Associated with geothermal activity?	Description
Suswa Southeast Slope 1	Suswa (5)	4	No*	Poorly lithified, argillaceous red and buff ochres associated with weathered volcanic ash and pumice. *Active fumaroles observed 500 m NNE at locality 2 (samples not analyzed).
Eburru Steam Condenser 1	EVC (2)	3	Yes	Poorly to moderately lithified, argillaceous, deep red and purple ochres associated with weathered pumice.
Eburru Steam Condenser 2	EVC (2)	4	Yes	Yellow, orange, red, purple, and green ochreous clays. Unlithified through moderately lithified.
Eburru Roadside Deposit	EVC (2)	2	Yes	Yellow and orange-red unlithified argillaceous ochres.
Eburru Crater	EVC (2)	7	Yes	Yellow, orange, red, green, gray, and black clays. Predominantly unlithified with rare well-lithified claystone. Associated with obsidian and weathered pumice and ash.
Moshi ya Maji	EVC (2)	4	Yes	Unlithified red ochreous clays associated with obsidian, rhyolite, and weathered pumice. This is also the location of an obsidian quarry (site GsJj82) referred to as “Eburu/GilGil Elmenteita Junction” by Coleman et al. (2008).
Hells Gate North Road Quarry	GOVC (3)	2	No	Moderately lithified yellow, orange, red, pink, and mauve argillaceous ochre. Associated with obsidian and pumice blocks.
Hells Gate Park Olkaria Gate	GOVC (3)	5	No	Moderately to well-lithified white, pink, orange, and red clays associated with outcrop containing various pyroclastic rocks.
Olomayiana Sabuk	GOVC (3)	7	Yes	Unlithified through moderately lithified gray, red, and purple ochreous clays and argillaceous volcanic soil.
Narasha	GOVC (3)	5	Yes	Poorly through moderately lithified yellow and red ochreous clays with white and gray mottling.

4.2. Sample preparation

Elemental characterization of each sample was done using Homogenized Ochre Chip (HOC) LA-ICPMS (Zipkin et al., 2015). This technique, first developed by Green and Watling (2007) and later modified by Zipkin et al. (2015), entails low temperature drying and manual homogenization of ochre by grinding with an agate mortar and pestle to a particle size of approximately one micrometer, and then dispersing it in a glue or epoxy binder that does not contain appreciable amounts of any elements of interest.

Once the epoxy and ochre mixture has set, chips are removed and embedded in epoxy for polishing and ablation. The HOC sample preparation technique is especially appropriate for use in LA-ICPMS studies of ochre. The more typical approach of ablating a polished solid rock sample is often not suitable for use with friable or wholly unlithified ochre samples of the type frequently encountered during this study. The only caveat to the advantages of this technique is that the elemental concentrations yielded cannot be considered absolute values for the composition of the ochre sources because the samples have been diluted with a binder. However, as long as the same preparation technique is used for all specimens there is no reason to expect that this will have deleterious effects on the statistical analysis of elemental fingerprint data.

The HOC preparation procedure used here was the same as that described in Zipkin et al. (2015) with the exception that Struers EpoFix epoxy was used as the binder rather than the Lineco neutral pH adhesive that was used previously. EpoFix is an epoxy composed entirely of carbon, hydrogen, oxygen, and nitrogen and when cured it is more suitable for polishing than Lineco neutral pH adhesive-containing HOCs. HOCs were embedded in 25 mm diameter epoxy discs, cured for at least eight hours, and then sequentially polished using 23 μm and 9 μm silicon carbide, 3 μm diamond film, and 1 μm alumina with ultrasonic cleaning in distilled water between each step. Each disc can hold up to ~60 HOCs (each ~4 mm^2), permitting efficient consecutive ablation of many samples and eliminating individual sample changing in the laser ablation sample cell, which can take up to 30 min to equilibrate after a sample change.

HOC samples are suitable for both spot and raster laser ablation. In the case of spot ablation, which was used here, we consider it most effective to obtain multiple ablations at different locations on each HOC in order to obtain a more representative data set for each specimen. In contrast to a spot analysis technique such as LA-ICPMS, INAA is a bulk sample method that yields compositional data for tens to hundreds of milligrams of sample material, albeit with fewer elements measured than with LA-ICPMS. INAA has previously been used effectively to discriminate among ochre sources on the basis of minor and trace element composition (Popelka-Filcoff et al., 2007; Eiselt et al., 2011; Zipkin et al., 2015). In an LA-ICPMS study it is possible by averaging the results of multiple ablations to obtain a mean elemental fingerprint for each sample that approximates a bulk analysis and increases the likelihood of distinguishing among sources by reducing "noise" in the dataset from intra-HOC heterogeneity. Each HOC in this study was ablated approximately five times, depending on the visibility of suitable locations for ablation and ability to adjust the laser to an appropriate focus depth. The results of individual ablations are presented in Table S1 and the means derived from these data in Table S2 (means calculation in tab 1 of Table S2, means only for statistical analysis in tab 2). Two ablations, one for sample KEN033 and one for sample KEN059, failed to yield usable data and are not included in Table S1 or S2.

4.3. LA-ICPMS analyses

The in situ LA–ICPMS analyses were done at the MicroAnalysis Facility – Bruneau Innovation Centre (MAF–IIC) at the Memorial University of Newfoundland using a Finnigan Element XR, a high-resolution double-focusing magnetic-sector inductively coupled plasma mass spectrometer (HR-ICPMS), coupled to a GeoLas 193 nm Excimer laser system. The specific methods for collection and processing of ICPMS data with this apparatus have previously been described in Zipkin et al. (2015) and were used again here with the modifications noted below.

A laser spot diameter of 79 μm was used for ablations of all ochre samples while a 49 μm spot was used for secondary standard reference materials NIST 612 and USGS BCR-2G, and 30 μm for the NIST 610 primary calibration material. The laser energy density used for all ablations was 3 J/cm^2 with a laser repetition rate of 8–10 Hz. Time-resolved intensity data were acquired by peak-jumping in a combination of pulse-counting and analog modes, depending on signal strength, with one point measured per peak. The LA-ICPMS data were acquired and viewed graphically as counts per second (CPS) vs. time. As the data were collected, the plot was refreshed at rapid time intervals to approximate a real-time view of the data acquisition. The ICP-MS was run for about 40 s before the laser aperture was opened to collect adequate background readings. Since the laser ablates into the sample over time, the x-axis time on the data acquisition plot is a proxy for depth as well as time. Thus, if an analyzed grain contained an inclusion within the analytical volume, the inclusion was detected as spike in the monitored constituent isotopes. In this case, the time interval integrated was selected so as to avoid the "contamination" effect of the inclusion, and thus obtain the real signal of the HOC analyzed.

A total of 40 elements were measured using LA-ICPMS. The Limits of Detection (LOD) for each element, shown in Table S1, were calculated in Iolite (Paton et al., 2011) separately for each element and each ablation using the method described in Zipkin et al. (2015). The results of each ablation in ppm were compared to the relevant LOD. Four elements analyzed, Li, Co, Ni, and Cu, were found to have an excessive number ($\geq$10) of below LOD observations; those elements were excluded from all statistical analyses. Table S2 shows the individual ablation (tab 1) and sample mean results (tab 2) for the 36 remaining elements that were available for statistical analysis. The exclusion of Li, Co, Ni, and Cu removed the majority of below LOD measures from the data set. For the nine remaining below LOD measurements, which occurred for Ca, Sc, V, and Cr and are highlighted in Table S2, the element concentrations were converted to zero before the calculation of the sample means. Mean element concentrations for each sample were used in all of the statistical analyses described below.

4.4. Electron Probe Microanalyzer (EPMA) analyses

The iron content was measured for each HOC using a JXA-8900 SuperProbe EPMA located at the University of Maryland at College Park, Advanced Imaging and Microscopy Laboratory. The following conditions were employed for the analyses: accelerating voltage of 15 kV, sample current of 25 nA, and a beam diameter of 20 microns. Natural magnetite, ilmenite and hornblende were used as standards for determining Fe concentrations (depending on the Fe count rates). Raw x-ray intensities were corrected using standard ZAF techniques. EPMA measurements were made at five locations on each HOC, adjacent to the previously acquired ablation craters from LA-ICPMS, and averaged to obtain a mean iron value used which was used for the reduction of all ICPMS data associated with that HOC.

4.5. Data analysis methods

All statistical analyses were done with JMP 11 software (SAS Institute Inc. 2013) using the multivariate analysis package. Principal Component Analyses (PCAs) were initially run to visualize the maximum extent of variation within the data set but were ineffective in discriminating among samples grouped by source or volcanic complex. Instead, Canonical Discriminant Analyses (CDAs), sometimes referred to as discriminant function analyses, were used to distinguish among sample groups. CDAs are advantageous for this purpose relative to PCAs because they maximize only inter-

group variation and not overall variation as in a PCA (Glascock, 1992; Zipkin et al., 2015). Like PCA, CDA is a dimension reduction technique that transforms multiple independent variables (element concentrations) into a linear combination of those variables; the discriminant or canonical function. The number of functions that may be generated is equal to the number of categorical groupings minus one. Thus, all CDAs done for this data set using volcanic center as the categorical variable involve two functions. When data points are grouped according to the ten sampled sources there may be as many as nine discriminant functions, though the first two still describe most of the variance. These functions can be used as the x and y axes of a bivariate plot (biplot) to visualize where each ochre sample plots with respect to the elemental variables included in the canonical functions, the multivariate mean (centroid) for each group, and the 95% confidence level ellipse (*not* a density ellipse) used to illustrate the statistical confidence for sample assignment to each group.

All CDAs used element (ppm) and oxide (wt%) concentrations that were not log transformed or normalized to the Fe content, as has sometimes been done in other ochre elemental characterization studies (e.g., Popelka-Filcoff et al., 2007; Eiselt et al., 2011). Although CDA makes several assumptions about the datasets used, including homogeneity of within-group covariance, linearity, similarity of sample size across groups, and multivariate normality, this technique has long been treated as relatively robust to violations of these assumptions in archaeological statistics (Wynn and Tierson, 1990; Baxter, 1994, p. 188). Data transformations such as base 10 or natural logarithm transformation are used frequently in archaeometry when datasets exhibit great deviation from a multivariate normal distribution. We tested the multivariate normality of our LOD corrected but otherwise unmodified dataset of mean elemental concentrations with the Henze–Zirkler empirical characteristic function test (Henze and Zirkler, 1990) using the MVN statistical package for the R programming environment (Korkmaz et al., 2014). A review of tests of multivariate normality (Mecklin and Mundfrom, 2004) identified the Henze–Zirkler test as the most mathematically consistent test available for a wide range of scenarios. The resulting p-value ($p = 0.0868$) indicates that our dataset does not deviate significantly from multivariate normality at 95% confidence. In light of the preliminary nature of the statistical analyses presented below in Section 5, in which we only attempt to discriminate among ochre sources and do not seek to assign ochres of unknown origin to a source group, we chose to not transform or standardize the ochre elemental characterization data. This decision made it considerably easier to interpret the role of each elemental variable in our analyses.

Elemental variables were added to each CDA model in a stepwise manner until it was possible to distinguish among all sample groups, unless otherwise noted in Section 5. Variables were entered consecutively in order of descending significance to the model (forward stepwise selection). More specifically, an analysis of covariance test was calculated in JMP in which the elemental variable under consideration was the response, the variables already entered into the discriminant model were predictors, and the group variable (ochre source or volcanic center) was a predictor. The test was performed for each variable not yet entered into the model and calculated a test statistic (the F-ratio, which has an F-distribution under the null hypothesis) and associated p-value for the group variable, indicating each variable's effect upon group discriminatory power. At each step, the variable with the smallest p-value was added to the model. Each time a new variable was entered into the model the F-ratios and p-values for the variables not yet included were automatically recalculated. This test was used to identify redundant or ineffective elements. Determining when the source groups have been clearly distinguished at the level that satisfies the PP can most easily be done by visualizing each group's 95% confidence ellipse in a biplot as described above, ensuring that no ellipses overlap, and that few or no samples plot within an incorrect group ellipse.

5. Results and discussion

5.1. Distinguishing among ochre sources at the regional (i.e., volcanic center) scale

During the August 2012 field season a total of 43 ochre samples were collected from ten sources and were analyzed by LA-ICPMS (Table 2, Table S3). These include five sources associated with the Eburru Volcanic Complex, four with the Greater Olkaria Volcanic Complex, and one with the Suswa Volcano near Soit Amut. In light of the distinct eruptive products and separate magma supplies for the three volcanic centers discussed previously, we began our analysis at the regional scale where the Provenience Postulate seemed most likely to be upheld.

When the ochre samples are identified by volcanic center and not individual source, it is possible to use stepwise CDA to create non-overlapping 95% confidence ellipses for the three centers, with no samples plotting within an incorrect ellipse, using just six variables: SiO_2, Sc, Hf, Ta, Th, and U. In a bivariate plot of this discriminant analysis (Fig. 3), canonical function 1 clearly distinguishes between the Eburru and Olkaria source groups, while canonical function 2 separates Suswa from the other two complexes. Canonical function 1 explains 82.1% of the variance in the model and is highly significant for discriminating among categories ($p < 0.0001$). Canonical function 2 explains the remaining 17.9% of variance and is also significant ($p = 0.0003$). Because only six elements were used to generate these canonical functions it is relatively straightforward to interpret which elements are discriminating among the volcano complexes graphically using the variable rays plotted on Fig. 3. The direction of each ray indicates the degree of association for that variable with the two canonical functions, as measured by the scoring coefficient for each function. More specifically, the standardized scoring coefficients for each elemental variable are indicative of that element's unique (partial) contribution to canonical function 1 or 2, with larger magnitude coefficients indicative of a greater contribution regardless of sign. Canonical function 1, which accounts for most of the variance in the model, may be interpreted as being primarily driven by Sc (standardized scoring coefficient 1.48), Hf (−2.77), and Th (2.09), while the greatest partial contributions to canonical 2 are from Hf (2.40), Ta (−1.97), and U (0.69). While technically effective in that this CDA yielded non-overlapping confidence ellipses, most of the individual ochre samples are highly dispersed outside of their appropriate confidence ellipse. In a sourcing study of ochre artifacts of unknown origin, this discriminant analysis would likely yield many misclassified specimens.

Next we sought to drive the centroids of the three groups farther apart by adding more variables to our model. In Fig. 4 biplot ochre samples are grouped by volcanic complex according to a CDA that simultaneously evaluated all 36 available elemental variables (excluding Li, Co, Ni, and Cu, as noted in Section 4.3). The 95% confidence ellipses for the three volcanic complex groups are clearly distinguished from one another. Despite a fair amount of scatter of individual samples outside their associated ellipse there is strong clustering of data points and no samples are assigned to an incorrect group. Canonical function 1 explains 91.2% of variance and is significant ($p = 0.0012$) while canonical function 2 explains the remaining 8.8% of variance and is not significant ($p = 0.1689$). Notably, if the y-axis in Fig. 4 was collapsed and the groups only plotted according to canonical function one, all three groups would

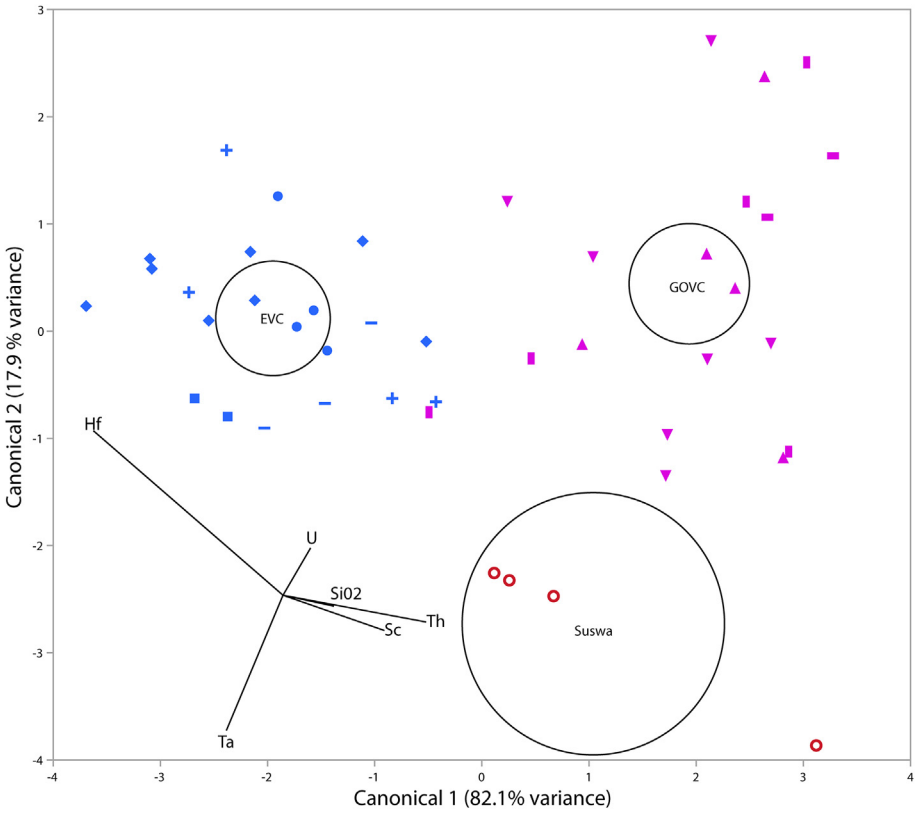

Fig. 3. Bivariate plot of a CDA constructed with sample means for 6 elements and oxides: SiO_2, Sc, Hf, Ta, Th, and U using the linear, common covariance method. All samples are grouped by volcanic complex with the 95% confidence ellipse shown for each group. Source Legend: ○ Suswa, ● Moshi ya Maji, ◆ Eburru Crater, ■ Eburru Roadside Deposit, − Eburru Steam Condenser 1, + Eburru Steam Condenser 2, ▌Hells Gate Park Olkaria Gate, – Hells Gate North Road Quarry, ▼ Olomayiana Sabuk, ▲ Narasha. These symbols are used to represent the sources in Figs. 3–10.

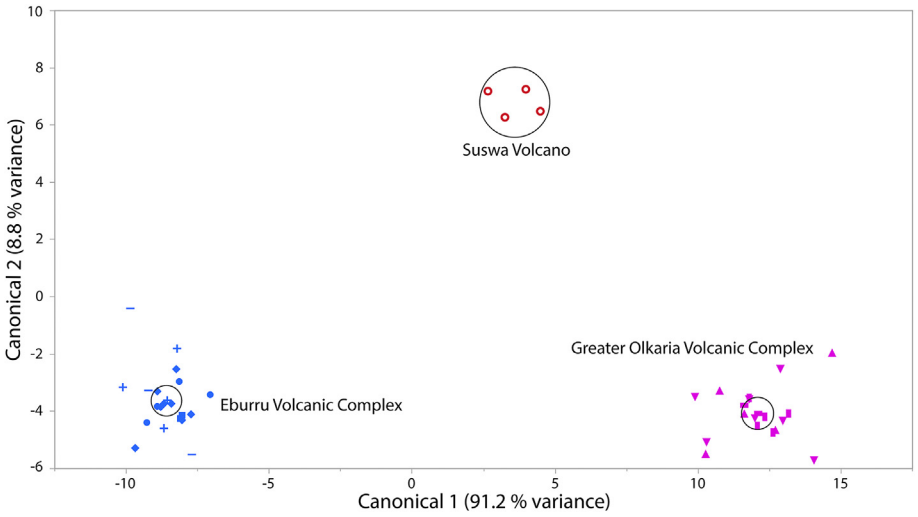

Fig. 4. Bivariate plot of a CDA constructed with sample means for 36 elements and oxides: MgO, SiO_2, P_2O_5, CaO, Sc, TiO_2, V, Cr, MnO, Zn, As, Sr, Y, Zr, Nb, Sn, Ba, La, Ce, Pr, Nd, Sm, Eu, Gd, Tb, Dy, Ho, Er, Tm, Yb, Lu, Hf, Ta, Pb, Th, and U using the linear, common covariance method. All samples are grouped by volcanic complex with the 95% confidence ellipse shown for each group.

still be distinguished. Visualizing variable loadings onto the canonical functions using biplot rays is not efficient when so many variables are considered.

Standardized scoring coefficients for canonical function 1 indicate a strong inverse association with the elements Gd (−153.1) and Ho (−127.5) and a moderate inverse association with Yb (−28.9), Pr (−26.9), and Lu (−13.7). Canonical function 1 has a strong direct association with Sm (93.5), Tm (73.2), Tb (54.0), Y (53.2), Dy (36.5), Nd (21.1), Er (15.3). These variables are overwhelmingly driving the discriminatory power of canonical function 1 with most other variables exhibiting scoring coefficients an order of magnitude smaller. More importantly, all of these variables are Rare Earth Elements (REEs). The 15 lanthanide REEs as a group tend to behave in a consistent manner during geologic processes owing to their

similar electronic configuration and small range in ionic radii from La to Lu. Sc and Y are also included among the REEs because they exhibit broadly similar chemical behavior to and often occur in the same ore deposits as the lanthanides (Rollinson, 1993). Canonical function 1 is largely tracking the variance for 12 of the 17 REEs. This is notable in light of the fact that the CDA shown in Fig. 3 only used one REE variable, Sc, which is not particularly important to canonical function 1 in Fig. 4 (standardized scoring coefficient 1.5). A likely explanation for this is that when evaluated alongside the other REEs, particularly Y, which exhibits chemical behavior similar to Sc, the discriminatory power of Sc becomes redundant. This interpretation is further supported by stepwise CDA with backward variable elimination. If all 36 variables are evaluated simultaneously, as in Fig. 4, and variables are removed stepwise in order of increasing significance then at 33 elements included canonical 1 remains significant ($p < 0.0001$) and canonical 2 becomes significant ($p = 0.0418$). The three elements removed to achieve significance for canonical function 2 are Sc, Ce, and Lu. These three elements are likely redundant to the discriminatory power of some of the other REEs and their inclusion adds noise to the model.

5.2. The significance of REE composition at the regional scale

To further investigate the significance of the rare earths for upholding the Provenience Postulate at the regional scale, chondrite normalized REE plots (spider plots) were generated using the IgPet (Rockware, Inc.) software program. Spider plots visualize the REE fingerprint of samples and facilitate efficient detection of any notable anomalies. All spider plots used sample mean REE values and were normalized to the chondrite values reported by Sun and McDonough (1989). Figs. 5–7 show chondrite normalized (Sun and McDonough, 1989) REE plots of mean concentrations of the lanthanide REEs measured in each sample, grouped by volcanic complex. The most striking observation, in light of the significance of REEs for discriminant analysis, is the apparent similarity between all three volcanic complexes. All volcanic centers generally show progressive depletion in concentration from light to heavy REEs (left to right) with a relatively flat heavy REE profile. The EVC ochre samples (Fig. 6) exhibit the greatest range of REE concentrations relative to the other volcanic centers but most of these still follow same broad pattern. If graphed on the same plot, the ochre samples from all three volcanic centers would overlap to such a degree as to be largely indistinguishable but this is largely due to the clutter of 43 lines of data and the amount of variability within each complex.

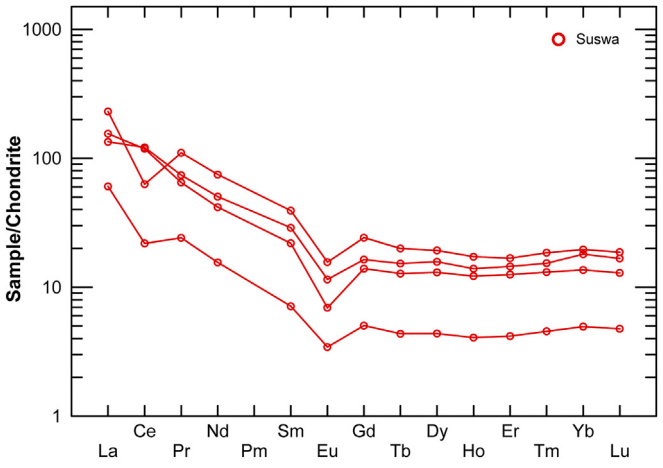

Fig. 5. Chondrite normalized (Sun and McDonough, 1989) REE spider plot of sample means for the Suswa volcano. Note that Pm was not measured in this study. Y-axis is log scaled.

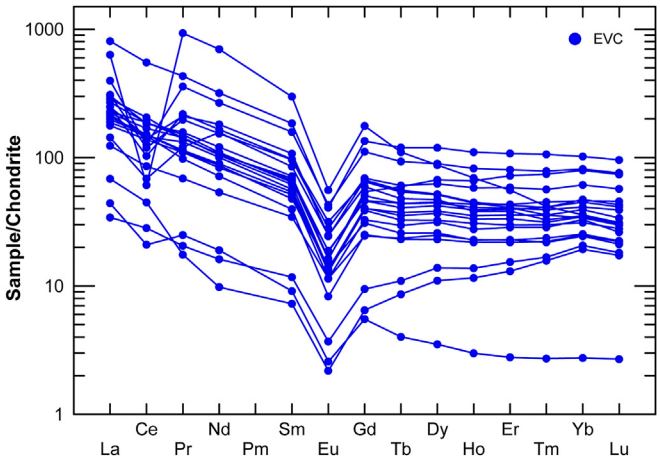

Fig. 6. Chondrite normalized (Sun and McDonough, 1989) REE spider plot of sample means for the Eburru Volcanic Complex. Y-axis is log scaled.

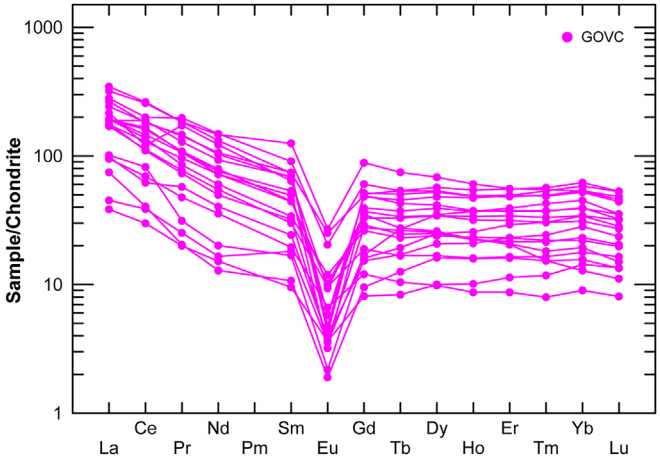

Fig. 7. Chondrite normalized (Sun and McDonough, 1989) REE spider plot of sample means for the Greater Olkaria Volcanic Complex. Y-axis is log scaled.

A clearer picture of the relevance of the REEs to discriminant analysis emerges when only the overall mean REE concentrations for each volcanic center are plotted (Fig. 8). In Fig. 8 it is clear that there are distinctions between the three volcanic centers despite their common trend in light to heavy REE depletion. For example, Mt. Suswa exhibits substantially lower mean heavy REE (Tb, Dy, Ho, Er, Tm, Yb, and Lu) concentrations than the other two volcanic centers. Some of the light REEs, particularly Pr and Nd, appear to distinguish the EVC from the GOVC and Suswa. When evaluated in a CDA without the other measured elements, the REEs are partially effective at upholding the Provenience Postulate. In an analysis using the 16 measured REEs (Pm was not measured by LA-ICPMS) to discriminate among volcanic groups the confidence ellipses in the resulting plot are non-overlapping but individual samples plot well outside of their associated ellipse and some are incorrectly assigned to the wrong volcanic complex (Fig. S1). The REEs may be necessary for effective group discrimination in some analyses but they are not sufficient on their own. Additional variables, as in Fig. 4, or a smaller number of mostly non-REE variables, as in Fig. 3, are required.

A second notable point illustrated by Figs. 5–8 is that every ochre sample has a negative Eu anomaly ranging from moderate to

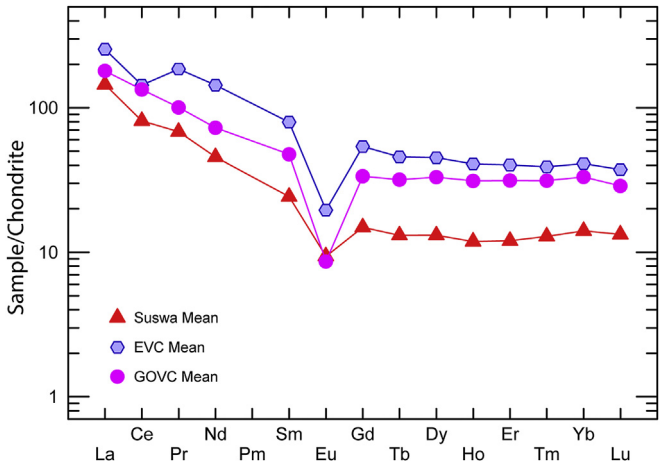

Fig. 8. Chondrite normalized (Sun and McDonough, 1989) REE spider plot of overall means for all samples analyzed from each volcanic center. Y-axis is log scaled.

marked depletion of Eu relative to Gd and Sm. Europium anomalies are typically expressed as a ratio between the chondrite normalized value measured in a sample (Eu(n)) and the expected value (Eu(n)*). Anomalies were calculated as $Eu(n)/Eu(n)^*$ where $Eu(n)^*$ is equal to $(Gd(n) + Sm(n))/2$. Eu anomalies are well-documented phenomena caused by the fact that while all lanthanide REEs are stabilized as trivalent ions, Eu can also occur as a divalent ion (Weill and Drake, 1973; Rollinson, 1993) and as such partition onto the divalent Ca site in plagioclase. Another REE phenomena, cerium anomalies, can occur because Ce may form Ce^{3+} or Ce^{4+} ions. The additional valence leads to Eu frequently behaving differently during rock formation processes than its near neighbors in the periodic table, Sm and Gd. Table S4 lists the Eu anomaly for each sample based on its chondrite normalized mean Gd, Eu, and Sm concentrations and Fig. S2 shows the distribution of the anomalies grouped by source and volcanic center. $Eu(n)/Eu(n)^*$ ranges from 0.069 to 0.565 with an overall mean of 0.294 and a standard deviation of 0.111. Broadly speaking, the four samples from the Suswa volcano showed the mildest negative anomalies ($\bar{x}_{Suswa} = 0.488$), while the EVC samples exhibited fairly consistent moderate anomalies ($\bar{x}_{EVC} = 0.308$) and the GOVC samples varied from moderate to extreme depletion ($\bar{x}_{GOVC} = 0.237$). An ANOVA test ($\alpha = 0.05$, $p < 0.0001$) and nonparametric Wilcoxon rank-sum test ($\alpha = 0.05$, $p = 0.0021$) confirm that significant differences in Eu anomalies exist among the volcanic centers.

One explanation for the prevalence of negative Eu anomalies in our data set is suggested by a study of the geochemistry of ferruginous fumarole deposits in the Valley of Ten Thousand Smokes, Alaska (Papike et al., 1991). In that study, fumarolic gas apparently induced leaching of plagioclase feldspar from a dacite-rich ash flow sheet, resulting in negative Eu anomalies in the altered protolith. This is a less than perfect comparison because the same altered samples that showed a negative Eu anomaly were also depleted in Fe_2O_3, in some samples to less than 1%, which is below the concentration generally necessary to stain a rock red and make it suitable for use as pigment. In a study of hydrothermal alteration of basaltic rock in the Los Azufres geothermal field, Mexico, Torres-Alvarado et al. (2007) reported a remarkably strong positive Eu anomaly in the hydrothermally altered rock and tentatively attributed this to the concentration of Eu incorporated in hydrothermal epidote after its release from plagioclase in the basalt. The authors further noted that their findings were likely unique to the conditions of that geothermal field and should not be extrapolated elsewhere. For our study area, Ren et al. (2006) noted that within the EVC rocks of the Eburru Trachyte Formation and the Eastern Eburru Pantellerite Formation exhibit deep negative Eu anomalies. While some of our ochre samples derive from the Eburru Pumice Formation, which was not analyzed by Ren and colleagues, several samples are from areas mapped as the Eburru Pantellerite Formation by Clarke et al. (1990). Further geochemical and mineralogical investigations of the ochreous deposits of the CKPP, and the volcanic parent rocks from which they have been altered, are required to elucidate the specific processes that govern their REE fingerprints.

5.3. Distinguishing among ochre at the local (source-specific) scale

In order to test the Provenience Postulate at the local scale, we conducted further discriminant analyses with samples grouped by individual source rather than by volcano complex. In contrast to the small number of elements (six) required to distinguish among ochre sources at the volcanic center scale (Fig. 3), the minimum number of variables required to produce non-overlapping confidence ellipses for all ten source groups is 33 elements (Fig. 9). The three elements with the least explanatory power for the model, Tb, Dy, and Lu, were not included. Canonical function 1 explains 83% of variability ($p < 0.0001$) while canonical function 2 explains an additional 10.4% ($p = 0.0021$). In Fig. 9 it is evident that canonical function 1 actually distinguishes among most of the sources successfully. This function is primarily driven by the elements Sm (standardized scoring coefficient 240.9), Gd (−135.9), Ho (−441.6), Tm (210.8), and Yb (−232.8), all with scoring coefficients an order of magnitude greater than the other elements used to build the function. Which variables ultimately prove effective for group discrimination is dependent upon how group membership for samples is assigned in a given CDA: regional groups with samples categorized by volcanic center or local groups with the same samples categorized by individual ochre deposits. Fig. 9 also shows that the sources associated with each volcanic center do not cluster together, indicating that there is a considerable amount of variability within each volcanic center. Some sources may have more in common with deposits at other centers than with sources associated with the same volcano. Ochre sources associated with a single volcanic center could be derived from different eruptive products separated by thousands of years of time and weathering.

The discriminant analyses illustrated in Figs. 3, 4, and 9 consider all ochre sources in our study area simultaneously. A perhaps more realistic scenario in an actual provenance study of archaeological ochre would be a narrower focus on probable sources. The characterization of mineral compositions by powder XRD or Raman spectroscopy and the quantification of ochre color by UV–vis–NIR spectroscopy could be used to exclude unlikely sources prior to running any discriminant analyses with elemental data. Figs. 10 and 11 illustrate stepwise CDAs of samples grouped by individual sources within the Eburru and Olkaria complexes, respectively. In contrast to the previous discriminant analyses of all sources, when only a single volcano complex is examined far fewer variables are required to distinguish among sources: MgO, SiO_2, P_2O_5, Sc, V, MnO, Zn, Sr, Zr, Sn, La, and Ta for the EVC sources and MgO, MnO, As, Sr, Zr, Nb, La, Ce, Sm, and Hf for the GOVC sources. The smaller number of variables required for intra-complex source discrimination is notable because analyses such as the CDA presented in Fig. 9 almost certainly suffer from model overfitting due to the large number of variables relative to sample count.

One of the goals of this study was to identify which elements most effectively distinguish among ochre sources and ochre source-containing volcano complexes in this part of Africa. We have already addressed this from the perspective of stepwise discriminant function analysis. Another approach, used in some

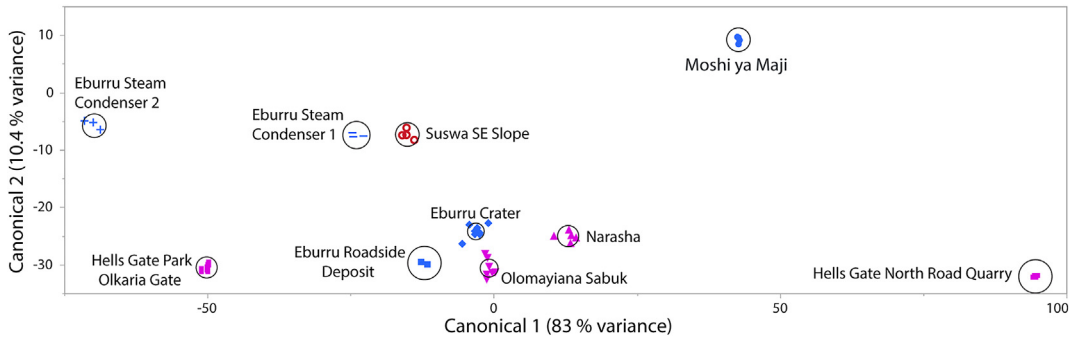

Fig. 9. Bivariate plot of a CDA constructed with sample means for 33 elements and oxides: MgO, SiO_2, P_2O5, CaO, Sc, TiO_2, V, Cr, MnO, Zn, As, Sr, Y, Zr, Nb, Sn, Ba, La, Ce, Pr, Nd, Sm, Eu, Gd, Ho, Er, Tm, Yb, Hf, Ta, Pb, Th, and U using the linear, common covariance method. All samples are grouped by individual source with the 95% confidence ellipse shown for each source.

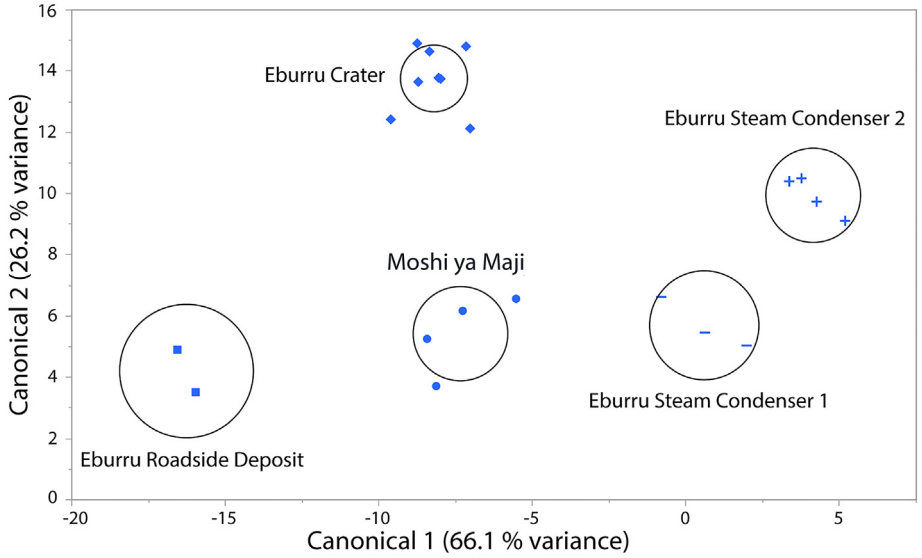

Fig. 10. Bivariate plot of a CDA for sources within the Greater Olkaria Volcanic Complex using the minimum number of variables required to discriminate among sources. CDA constructed with 10 elements and oxides: MgO, MnO, As, Sr, Zr, Nb, La, Ce, Sm, and Hf using the linear, common covariance method. All samples are grouped by individual source with the 95% confidence ellipse shown for each source.

provenience studies of ochre pigments such as Kiehn et al. (2007), Popelka-Filcoff et al. (2007, 2008), and Dayet et al. (2015), emphasized consideration of only those elements that correlate positively with Fe content; these form the "Fe-oxide signature". Elements that correlate positively with iron content are believed to represent the trace element fingerprint of the iron oxide phases (hematite, goethite, etc.) that act as the chromophore for the ochre while those elements that negatively correlate with iron represent dilutant minerals such as quartz or various clays. There may be some basis for relying on the Fe-oxide signature in cases where ochre could have been modified by anthropogenic activities, such as deliberately diluting natural pigment with other materials or

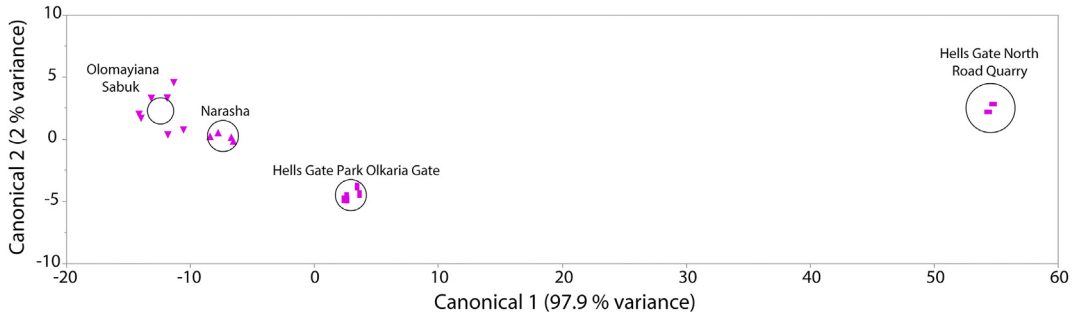

Fig. 11. Bivariate plot of a CDA for sources within the Eburru Volcanic Complex using the minimum number of variables required to discriminate among sources. CDA constructed with 12 elements and oxides: MgO, SiO_2, P_2O_5, Sc, V, MnO, Zn, Sr, Zr, Sn, La, and Ta using the linear, common covariance method. All samples are grouped by individual source with the 95% confidence ellipse shown for each source.

processing pigment with a grindstone. However, it is our opinion that excluding elements that negatively correlate with iron, without a clear rationale, is detrimental. A Pearson product-moment correlation for each element with mean iron content found eight elements that negatively correlate with iron: As, Ba, Ca, Mg, Si, Sr, Th, and U (Table S5). Although none of these elements had a significant negative correlation ($\alpha = 0.1$) we attempted to run discriminant analyses excluding these variables to determine if this had a negative impact on the ability to distinguish among sources. At the individual source level, we found that no combination of variables that excluded those eight elements could successfully generate non-overlapping confidence ellipses. At the volcanic center scale it was possible to separate the three groups, although with considerable dispersion of individual samples outside of their associated ellipse. This underscores the importance of not excluding any variables a priori; elements associated with naturally present dilutant minerals (e.g. clays) may form an important part of the fingerprint of the ochre as whole.

6. Conclusions

The overarching goal of this project was to determine the feasibility of using HOC-LA-ICPMS for provenance studies of ochre pigments derived from different sources within the Kenya Rift Valley. The results presented here show that this technique can discriminate among ochre deposits in the KRV at the volcanic center scale and at the scale of individual sources located, in some cases, as close as ~1–2 km from one another, and that inter-source trace element variations are greater than intra-source variations. Source discrimination should be considered more robust at the volcanic center scale owing to the greater numbers of samples per group relative to the low sample count for some individual sources. Analysis of more samples for each source and volcanic center will facilitate improved discriminant function building through cross-validation testing and will yield enhanced statistical stability through greater sample count relative to the number of elemental variables considered. In future provenance studies of ochre artifacts, residues, or rock art from the KRV, we will use additional analytic techniques to characterize ochre mineralogy and color prior to trace element characterization. The application of multiple complementary techniques for provenance analysis is exemplified by Dayet et al. (2015) study of ochre artifacts from Diepkloof Rock Shelter, South Africa, in which a combination of XRD, ICPMS, and ICP-OES was used.

Long-established elemental analysis techniques, particularly INAA, have also been demonstrated to be effective for sourcing ochreous minerals. However, the viability of using that technique to analyze cultural heritage artifacts is limited by the size of the bulk sample required and the limited number of neutron radiation sources available (Pollard et al., 2007). LA-ICPMS represents a widely accessible, minimally destructive, and less costly alternative (Speer, 2014) that is capable of measuring a comparable or greater range of elements (~30–34 elements for INAA, 30–40 elements for LA-ICPMS) for geologic samples, ochre artifacts, and ochre residues. This pilot study demonstrates the potential for using minimally destructive techniques to provenience mineral pigments in a region with an archaeological record rich in this material. The development of obsidian geochemistry databases for East Africa (Merrick and Brown, 1984; Negash et al., 2006; Coleman et al., 2008; Nash et al., 2011), with increasingly thorough coverage of sources, has greatly strengthened the ability of archaeologists to study material transport patterns in prehistory. Further survey, sampling, and elemental characterization of Kenyan ochre sources has the potential to do the same with the added benefit of enhancing our ability to interpret rock art sites and identify modern alterations to them. An expanded ochre source survey in the KRV was conducted in 2015 and 2016, and these samples are currently being analyzed. This field work was explicitly guided by cultural considerations and emphasized the sampling of ochre deposits preferentially exploited by Maasai and Samburu pastoralists for purposes such as self-adornment and rock art painting. The findings from this refined ethno-archaeometry approach to the study of ochre pigment use in Kenya will be presented in forthcoming publications.

Acknowledgements

Financial support for this research was provided by National Science Foundation (NSF) Graduate Research Fellowship 2011116368 (Zipkin), NSF Doctoral Dissertation Research Improvement Grant BCS-1240694 (Brooks and Zipkin), NSF IGERT DGE-0801634 (Center for the Advanced Study of Human Paleobiology), Wenner-Gren Foundation Dissertation Fieldwork Grant 8623 (Zipkin), and a Natural Sciences and Engineering Research Council of Canada Discovery Grant (Hanchar). Thanks to Alex Chafe for help with the Iolite data reduction at MUN and to Lin Ma for his help with the U-series analyses at UTEP. The two anonymous reviewers whose comments improved the final version of this manuscript have our gratitude. This project would not have been possible without the permission and support of the Government of Kenya and the National Museums of Kenya and the invaluable assistance of our Maasai guides Emmanuel Ole Keri, Elijah Ole Keri, and Sayialel Ole Manyara.

Appendix A. Supplementary data

Supplementary data related to this article can be found at http://dx.doi.org/10.1016/j.quaint.2016.08.032.

References

Allen, D.J., Darling, W.G., Burgess, W.G., 1989. Geothermics and Hydrogeology of the Southern Part of the Kenya Rift Valley with Emphasis on the Magadi Nakuru Area. British Geological Survey. No. SD/89/1.

Ambrose, S.H., 1984. Holocene Environments and Human Adaptations in the Central Rift Valley, Kenya (Ph.D. thesis). University of California, Berkeley.

Ambrose, S.H., 1998. Chronology of the Later Stone Age and food production in East Africa. Journal of Archaeological Science 25, 377–392.

Ambrose, S.H., 2007. Raiders of the lost art: implications of rock art forgery at Lukenya Hill, Kenya, for cultural and natural heritage protection strategies. In: Deacon, J. (Ed.), The Future of Africa's Past: Proceedings of Rock Art Conference, 2004, Nairobi. Trust for African Rock Art, Nairobi, pp. 128–132.

Aubert, M., 2016. Further comment on: "Uranium–thorium dating method and Palaeolithic rock art" by Sauvet et al. (2015, in press). Quaternary International. http://dx.doi.org/10.1016/j.quaint.2016.04.020.

Audouin, F., Plisson, H., 1982. Les ocres et leurs témoins au Paléolithique en France: enquête et expériences sur leur validité archéologique. Cahiers du Centre de Recherches Préhistoriques Paris 8, 33–80.

Baker, B.H., Mitchell, J.G., Williams, L.A.J., 1988. Stratigraphy, geochronology and volcano-tectonic evolution of the Kedong-Naivasha-Kinangop region, Gregory Rift Valley, Kenya. Journal of the Geological Society, London 145, 107–116.

Barham, L., 2002. Systematic pigment use in the Middle Pleistocene of South-Central Africa. Current Anthropology 43, 181–190.

Baxter, M.J., 1994. Exploratory Multivariate Analysis in Archaeology. Edinburgh University Press, Edinburgh.

Biggs, J., Anthony, E.Y., Ebinger, C.J., 2009. Multiple inflation and deflation events at Kenyan volcanoes, East African Rift. Geology 37, 979–982.

Bikiaris, D., Daniilia, S., Sotiropoulou, S., Katsimbiri, O., Pavlidou, E., Moutsatsou, A.P., Chryssoulakis, Y., 1999. Ochre-differentiation through micro-Raman and micro-FTIR spectroscopies: application on wall paintings at Meteora and Mount Athos, Greece. Spectrochimica Acta - Part A: Molecular and Biomolecular Spectroscopy 56, 3–18.

Blackburn, R.H., 1971. Honey in Okiek Personality, Culture and Society (Ph.D. thesis). Michigan State University, Ann Arbor.

Boivin, N., 2004. Rock art and rock music: petroglyphs of the south Indian Neolithic. Antiquity 78, 38–53.

Bower, J.R.F., Nelson, C.M., Waibel, A.F., Wandibba, S., 1977. The University of Massachusetts' Later Stone Age/Pastoral 'Neolithic' comparative study in central Kenya: an overview. Azania 12, 119–146.

Brandt, S.A., Weedman, K., 2002. Woman the toolmaker: a day in the life of an Ethiopian woman who scrapes hides the old-fashioned way. Archaeology 55, 50–53.
Brooks, A.S., Yellen, J., Zipkin, A.M., Dussubieux, L., Potts, R., 2016. Early worked ochre in the Middle Pleistocene at Olorgesailie, Kenya. In: Abstracts of the SAA 81st Annual Meeting, 53.
Bu, K., Cizdziel, J.V., Russ, J., 2013. The source of iron-oxide pigments used in Pecos River style rock paints. Archaeometry 55, 1088–1100.
Burdukiewicz, J.M., 2014. The origin of symbolic behavior of Middle Palaeolithic humans: recent controversies. Quaternary International 326, 398–405.
Cavallo, G., Fontana, F., Gonzato, F., Guerreschi, A., Riccardi, M.P., Sardelli, G., Zorzin, R., 2015. Sourcing and processing of ochre during the late Upper Palaeolithic at Tagliente rock-shelter (NE Italy) based on conventional X-ray powder diffraction analysis. Archaeological and Anthropological Sciences 1–13. http://dx.doi.org/10.1007/s12520-015-0299-3.
Chalmin, É., Castets, G., Delannoy, J.J., David, B., Barker, B., Lamb, L., Soufi, F., Pairis, S., Cersoy, S., Martinetto, P., Geneste, J.M., 2016. Geochemical analysis of the painted panels at the "Genyornis" rock art site, Arnhem Land, Australia. Quaternary International. http://dx.doi.org/10.1016/j.quaint.2016.04.003.
Chamberlain, N., 2006. Report on the rock art of south west Samburu District, Kenya. Azania 41, 139–157.
Chaplin, J.H., 1974. The prehistoric rock art of the Lake Victoria Region. Azania 9, 1–50.
Clarke, M.C.G., Woodhall, D.G., Allen, D., Darling, G., 1990. Geological, Volcanological and Hydrological Controls on the Occurrence of Geothermal Activity in the Area Surrounding Lake Naivasha, Kenya. Republic of Kenya, Ministry of Energy, Derry and Sons Ltd., Nottingham.
Coleman, M.E., Ferguson, J.R., Glascock, M.D., Robertson, J.D., Ambrose, S.H., 2008. A new look at the geochemistry of obsidian from East Africa. International Association for Obsidian Studies Bulletin 39, 11–14.
Conkey, M.W., Soffer, O., Stratmann, D., Jablonski, N.G., 1997. Beyond Art: Pleistocene Image and Symbol. California Academy of Sciences, San Francisco.
Cornell, R.M., Schwertmann, U., 2003. The Iron Oxides: Structure, Properties, Reactions, Occurrences and Uses, second ed. Wiley-VCH, Weinheim.
Coulson, D., 2006. Discoveries in Maasailand, Kenya. Trust for African Rock Art Newsletter 8, 6.
Dale, D., Ashley, C.Z., 2010. Holocene hunter-fisher-gatherer communities: new perspectives on Kansyore using communities of western Kenya. Azania 45, 24–48.
Darling, W.G., Griesshaber, E., Andrews, J.N., Armannsson, H., O'Nions, R.K., 1995. The origin of hydrothermal and other gases in the Kenya Rift Valley. Geochimica et Cosmochimica Acta 59, 2501–2512.
David, B., Geneste, J.M., Petchey, F., Delannoy, J.J., Barker, B., Eccleston, M., 2013. How old are Australia's pictographs? A review of rock art dating. Journal of Archaeological Science 40, 3–10.
Dayet, L., Le Bourdonnec, F.X., Daniel, F., Porraz, G., Texier, P.J., 2015. Ochre provenance and procurement strategies during the Middle Stone Age at Diepkloof Rock Shelter, South Africa. Archaeometry. http://dx.doi.org/10.1111/arcm.12202.
Dayet, L., Texier, P.J., Daniel, F., Porraz, G., 2013. Ochre resources from the Middle Stone Age sequence of Diepkloof Rock Shelter, Western Cape, South Africa. Journal of Archaeological Science 40, 3492–3505.
Deino, A.L., McBrearty, S., 2002. 40Ar/39Ar dating of the Kapthurin Formation, Baringo, Kenya. Journal of Human Evolution 42, 185–210.
Eerkens, J.W., Barfod, G.H., Vaughn, K.J., Williams, P.R., Lesher, C.E., 2014. Iron isotope analysis of red and black pigments on pottery in Nasca, Peru. Archaeological and Anthropological Sciences 6, 241–254.
Eerkens, J.W., Gilreath, A.J., Joy, B., 2012. Chemical composition, mineralogy, and physical structure of pigments on arrow and dart fragments from Gypsum Cave, Nevada. Journal of California and Great Basin Anthropology 32, 47–64.
Eiselt, B.S., Popelka-Filcoff, R.S., Darling, J.A., Glascock, M.D., 2011. Hematite sources and archaeological ochres from Hohokam and O'odham sites in central Arizona: an experiment in type identification and characterization. Journal of Archaeological Science 38, 3019–3028.
Erlandson, J.M., Robertson, J.D., Descantes, C., 1999. Geochemical analysis of eight red ochres from western North America. American Antiquity 64, 517–526.
Fiore, D., 2014. Archaeology of art: theoretical frameworks. In: Smith, C. (Ed.), Encyclopedia of Global Archaeology. Springer Science+Business Media, New York, pp. 436–449.
Furman, T., 2007. Geochemistry of East African rift basalts: an overview. Journal of African Earth Sciences 48, 147–160.
Glascock, M., 1992. Characterization of archaeological ceramics at MURR by neutron activation analysis and multivariate statistics. In: Neff, H. (Ed.), Chemical Characterization of Ceramic Pastes in Archaeology, Monographs in World Archaeology No. 7. Prehistory Press, Madison, pp. 11–26.
Global Volcanism Program, 2013. In: Venzke, E. (Ed.), Volcanoes of the World, v. 4.4.1. Smithsonian Institution. http://dx.doi.org/10.5479/si.GVP.VOTW4-2013. Accessed 04 Jan 2016.
Gosden, C., Marshall, Y., 1999. The cultural biography of objects. World Archaeology 31, 169–178.
Gramly, R.M., 1975a. Meat-feasting sites and cattle brands: patterns of rock-shelter utilization in East Africa. Azania 10, 107–121.
Gramly, R.M., 1975b. Pastoralist and Hunters: Recent Prehistory in Southern Kenya and Northern Tanzania (Ph.D. thesis). Harvard University, Cambridge.
Green, R.L., Watling, R.J., 2007. Trace element fingerprinting of Australian ocher using laser ablation inductively coupled plasma-mass spectrometry (LA-ICP-MS) for the provenance establishment and authentication of indigenous art. Journal of Forensic Sciences 52, 851–859.
Guth, A., Wood, J., 2014. Geological Map of the Southern Kenya Rift. Geological Society of America Digital Map and Chart Series 16, Sheet 1 (Geology of the Suswa Region, Kenya). The Geological Society of America, Boulder. http://dx.doi.org/10.1130/2014.DMCH016.
Haughton, P.D.W., Todd, S.P., Morton, A.C., 1991. Sedimentary provenance studies. Geological Society, London, Special Publications 57, 1–11.
Helwig, K., Monahan, V., Poulin, J., Andrews, T.D., 2014. Ancient projectile weapons from ice patches in northwestern Canada: identification of resin and compound resin-ochre hafting adhesives. Journal of Archaeological Science 41, 655–665.
Henshilwood, C.S., d'Errico, F., Watts, I., 2009. Engraved ochres from the Middle Stone Age levels at Blombos Cave, South Africa. Journal of Human Evolution 57, 27–47.
Henshilwood, C.S., d'Errico, F., Van Niekerk, K.L., Coquinot, Y., Jacobs, Z., Lauritzen, S.-E., Menu, M., García-Moreno, R., 2011. A 100,000-year-old ochre-processing workshop at Blombos Cave, South Africa. Science 334, 219–222.
Henze, N., Zirkler, B., 1990. A class of invariant consistent tests for multivariate normality. Communications in Statistics - Theory and Methods 19, 3595–3617.
Hirst, K.K., 2006. Provenience, Provenance, Let's Call the Whole Thing Off. Accessed 01 January 2016. http://archaeology.about.com/b/2006/05/16/provenience-provenance-lets-call-the-whole-thing-off.htm.
Hovers, E., Ilani, S., Bar-Yosef, O., Vandermeersch, B., 2003. An early case of color symbolism: ochre use by modern humans in Qafzeh Cave 1. Current Anthropology 44, 491–522.
Huntley, J., Brand, H., Aubert, M., Morwood, M.J., 2014. The first Australian synchrotron powder diffraction analysis of pigment from a Wandjina motif in the Kimberley, Western Australia. Australian Archaeology 78, 33–38.
Huntley, J., Watchman, A., Dibden, J., 2011. Characteristics of a pigment art sequence: Woronora Plateau, New South Wales. Rock Art Research 28, 85–97.
Jercher, M., Pring, A., Jones, P.G., Raven, M.D., 1998. Rietveld X-ray diffraction and X-ray fluorescence analysis of Australian Aboriginal ochres. Archaeometry 40, 383–401.
Johnson, R.W., 1969. Volcanic geology of Mount Suswa, Kenya. Philosophical Transactions of the Royal Society, London A 265, 383–412.
Joyce, R., 2012. From place to place: provenience, provenance, and archaeology. In: Feigenbaum, G., Reist, I. (Eds.), Provenance: an Alternate History of Art. Getty Research Institute, Los Angeles, pp. 50–62.
Joyce, R., 2013. When is authentic? Situating authenticity in the itineraries of objects. In: Guerds, A., Van Broekhoven, L. (Eds.), Creating Authenticity: Authentication Processes in Ethnographic Museums. Sidestone Press, Leiden, pp. 39–58.
Kamwendo, L.A., 2009. Childbirth experiences in Malawi. In: Selin, H., Stone, P.K. (Eds.), Childbirth Across Cultures, Science Across Cultures: the History of Non-Western Science 5. Springer Science+Business Media B.V, London and New York, pp. 235–244.
Keith, T.E.C., 1991. Fossil and active fumaroles in the 1912 eruptive deposits, Valley of Ten Thousand Smokes, Alaska. Journal of Volcanology and Geothermal Research 45, 227–254.
Keller, G.R., Prodehl, C., Mechie, J., Fuchs, K., Khan, M.A., Maguire, P.K.H., Mooney, W.D., Achauer, U., Davis, P.M., Meyer, R.P., Braile, L.W., Nyambok, I.O., Thompson, G.A., 1994. The East African rift system in the light of KRISP 90. Tectonophysics 236, 465–483.
KenGen, 2012. Olkaria IV (Domes) Geothermal Project in Naivasha District: Resettlement Action Plan for Olkaria IV Power Station. Accessed 08 February 2015. http://www.kengen.co.ke/userfiles/OLKARIA%20IV%20RAP%20FOR%20DISCLOSURE_JULY%20%202012.pdf.
Kiehn, A.V., Brook, G.A., Glascock, M.D., Dake, J.Z., Robbins, L.H., Campbell, A.C., 2007. Fingerprinting specular hematite from mines in Botswana, southern Africa. In: Glascock, M.D., Speakman, R.J., Popelka-Filcoff, R.S. (Eds.), Archaeological Chemistry: Analytical Techniques and Archaeological Interpretation. American Chemical Society, Washington, D.C, pp. 460–479.
Korkmaz, S., Goksuluk, D., Zararsiz, G., 2014. MVN: an R package for assessing multivariate normality. The R Journal 6, 151–162.
Kozowyk, P.R.B., Langejans, G.H.J., Poulis, J.A., 2016. Lap shear and impact testing of ochre and beeswax in experimental Middle Stone Age compound adhesives. PLoS One 11, e0150436. http://dx.doi.org/10.1371/journal.pone.0150436.
Kubai, R., Kandie, R., 2014. Structural geology of Eburru-Badlands geothermal project. Proceedings 5th African Rift Geothermal Conference. Arusha, Tanzania, pp. 1–9.
Lagat, J., 2003. Geology and the geothermal systems of the southern segment of the Kenya Rift. International Geothermal Conference. Reykjavik, Iceland, pp. 40–47.
Lagat, J., 2007. Hydrothermal alteration mineralogy in geothermal fields with case examples from Olkaria domes geothermal field, Kenya. In: Short Course II on Surface Exploration for Geothermal Resources. Lake Naivasha, Kenya, pp. 1–26.
Lawren, W.L., 1968. Masai and Kikuyu: an historical analysis of culture transmission. The Journal of African History 9, 571–583.
Leakey, M.D., 1983. Africa's Vanishing Art: the Rock Paintings of Tanzania. Hamilton, London.
Leakey, M.D., Leakey, L.S.B., 1950. Excavations at the Njoro River Cave. Clarendon Press, Oxford.
Lewis-Williams, D.D., 1987. Beyond style and portrait: a comparison of Tanzanian and southern African rock art. In: Vossen, R., Keuthmann, K. (Eds.), Contemporary Studies on Khoisan 2. Helmut Buske Verlag, Hamburg, pp. 93–139.

Lombard, M., 2005. Evidence of hunting and hafting during the Middle Stone Age at Sibudu Cave, KwaZulu-Natal, South Africa: a multianalytical approach. Journal of Human Evolution 48, 279–300.
Mabulla, A.Z., 2005. The rock art of Mara region, Tanzania. Azania 40, 19–42.
MacDonald, B.L., Hancock, R.G.V., Cannon, A., McNeill, F., Reimer, R., Pidruczny, A., 2013. Elemental analysis of ochre outcrops in southern British Columbia, Canada. Archaeometry 55, 1020–1033.
MacDonald, R., 1974. Nomenclature and petrochemistry of the peralkaline oversaturated extrusive rocks. Bulletin Volcanologique 38, 498–516.
MacDonald, R., Bagiński, B., 2009. The central Kenya peralkaline province: a unique assemblage of magmatic systems. Mineralogical Magazine 73, 1–16.
MacDonald, R., Kjarsgaard, B.A., Skilling, I.P., Davies, G.R., Hamilton, D.L., Black, S., 1993. Liquid immiscibility between trachyte and carbonate in ash flow tuffs from Kenya. Contributions to Mineralogy and Petrology 114, 276–287.
MacDonald, R., Scaillet, B., 2006. The central Kenya peralkaline province: insights into the evolution of peralkaline salic magmas. Lithos 91, 59–73.
Mackay, A., Welz, A., 2008. Engraved ochre from a Middle Stone Age context at Klein Kliphuis in the Western Cape of South Africa. Journal of Archaeological Science 35, 1521–1532.
Marean, C.W., Bar-Matthews, M., Bernatchez, J., Fisher, E., Goldberg, P., Herries, A., Jacobs, Z., Jerardino, A., Karkanas, P., Minichello, T., Nilssen, P., Thompson, E., Watts, I., Williams, H., 2007. Early human use of marine resources and pigment in South Africa during the Middle Pleistocene. Nature 449, 905–908.
Marshall, A.S., MacDonald, R., Rogers, N.W., Fitton, J.G., Tindle, A.G., Nejbert, K., Hinton, R.W., 2009. Fractionation of peralkaline silicic magmas: the greater Olkaria volcanic complex, Kenya Rift Valley. Journal of Petrology 50, 323–359.
Masao, F.T., 1979. The Later Stone Age and the rock paintings of central Tanzania. Studien zur Kulturkunde Wiesbaden 48, 1–311.
Matarrese, A., Di Prado, V., Poiré, D.G., 2011. Petrologic analysis of mineral pigments from hunter-gatherers archaeological contexts (Southeastern Pampean region, Argentina). Quaternary International 245, 2–12.
Mathis, F., Bodu, P., Dubreuil, O., Salomon, H., 2014. PIXE identification of the provenance of ferruginous rocks used by Neanderthals. Nuclear Instruments and Methods in Physics Research Section B: Beam Interactions with Materials and Atoms 331, 275–279.
McBrearty, S., Brooks, A.S., 2000. The revolution that wasn't: a new interpretation of the origin of modern human behavior. Journal of Human Evolution 39, 453–563.
McCall, G.J.H., Bristow, C.M., 1965. An introductory account of Suswa volcano, Kenya. Bulletin Volcanologique 28, 333–367.
Mecklin, C.J., Mundfrom, D.J., 2004. An appraisal and bibliography of tests for multivariate normality. International Statistical Review 72, 123–138.
Merrick, H.V., Brown, F.H., 1984. Obsidian sources and patterns of source utilization in Kenya and northern Tanzania: some initial findings. African Archaeological Review 2, 129–152.
Mioč, U.B., Colomban, P., Sagon, G., Stojanović, M., Rosić, A., 2004. Ochre decor and cinnabar residues in Neolithic pottery from Vinča, Serbia. Journal of Raman Spectroscopy 35, 843–846.
Mol, F., 1978. Maa: a Dictionary of the Maasai Language and Folklore. Marketing and Publishing Ltd., Nairobi.
Moyo, S., Mphuthi, D., Cukrowska, E., Henshilwood, C.S., van Niekerk, K., Chimuka, L., 2016. Blombos Cave: Middle Stone Age ochre differentiation through FTIR, ICP OES, ED XRF and XRD. Quaternary International 404, 20–29.
Mulvaney, D.J., 1978. Creativity in the Aboriginal past. In: Edwards, R. (Ed.), Aboriginal Art in Australia. Ure Smith, Sydney, pp. 11–20.
Mulvaney, K., 2013. Iconic imagery: Pleistocene rock art development across northern Australia. Quaternary International 285, 99–110.
Nash, B.P., Merrick, H.V., Brown, F.H., 2011. Obsidian types from Holocene sites around Lake Turkana, and other localities in northern Kenya. Journal of Archaeological Science 38, 1371–1376.
Nakamura, K., 2005. Adornments of the Samburu in Northern Kenya: a Comprehensive List. Center for African Studies, Kyoto University, Kyoto.
Neff, H., 2000. Neutron activation analysis for provenance determination in archaeology. In: Ciliberto, E., Spoto, G. (Eds.), Modern Analytical Methods in Art and Archaeology, Chemical Analysis Series, vol. 155. John Wiley & Sons, New York, pp. 81–133.
Negash, A., Shackley, M.S., Alene, M., 2006. Source provenance of obsidian artifacts from the Early Stone Age (ESA) site of Melka Konture, Ethiopia. Journal of Archaeological Science 33, 1647–1650.
Nowell, A., 2006. From a paleolithic art to pleistocene visual cultures (Introduction to two Special Issues on 'Advances in the Study of Pleistocene Imagery and Symbol Use'). Journal of Archaeological Method and Theory 13, 239–249.
Odak, O., 1977. Kakapeli and other recently discovered rock paintings in the western highlands of Kenya. Azania 12, 187–192.
Omenda, P.A., 2005. The geology and geothermal activity of the East African Rift System. In: Workshop for Decision Makers on Geothermal Projects and Management. Naivasha, Kenya, pp. 1–10. Accessed 05 January 2015. http://www.os.is/gogn/unu-gtp-sc/UNU-GTP-SC-01-03.pdf.
Omenda, P.A., 2008. Status of geothermal exploration in Kenya and future plans for its development. In: Short Course III on Exploration for Geothermal Resources. United Nations University Geothermal Training Program and KenGen, Lake Naivasha, Kenya, pp. 1–13. Accessed 16 January 2016. http://www.os.is/gogn/unu-gtp-sc/UNU-GTP-SC-10-0902.pdf.
Ouzman, S., 2010. Flashes of brilliance: San rock paintings of heaven's things. In: Blundell, G., Chippindale, C., Smith, B. (Eds.), Seeing and Knowing: Understanding Rock Art with and without Ethnography. Left Coast Press, Walnut Creek, California, pp. 11–35.
Papike, J.J., Keith, T.E.C., Spilde, M.N., Galbreath, K.C., Shearer, C.K., Laul, J.C., 1991. Geochemistry and mineralogy of fumarolic deposits, Valley of Ten Thousand Smokes, Alaska: bulk chemical and mineralogical evolution of dacite-rich protolith. American Mineralogist 76, 1662–1673.
Paton, C., Hellstrom, J., Paul, B., Woodhead, J., Hergt, J., 2011. Iolite: freeware for the visualisation and processing of mass spectrometric data. Journal of Analytical Atomic Spectrometry 26, 2508–2518.
Peile, A.R., 1997. Colours that cure. Hemisphere 23, 214–217.
Peterson, N., Lampert, R., 1985. A central Australian ochre mine. Records of the Australian Museum 37, 1–9.
Pollard, A.M., Batt, C.M., Stern, B., Young, S.M.M., 2007. Analytical Chemistry in Archaeology. Cambridge University Press, Cambridge.
Pollard, A.M., Bray, P.J., Gosden, C., 2014. Is there something missing in scientific provenance studies of prehistoric artefacts? Antiquity 88, 625–631.
Pons-Branchu, E., Fontugne, M., Michel, V., Valladas, H., 2015. Comment on: "Uranium–thorium dating method and Palaeolithic rock art" by Sauvet et al. (2015, in press). Quaternary International. http://dx.doi.org/10.1016/j.quaint.2015.10.015.
Popelka-Filcoff, R.S., Craig, N., Glascock, M.D., Robertson, J.D., Aldenderfer, M., Speakman, R.J., 2007. Instrumental neutron activation analysis of ochre artifacts from Jiskairumoko, Peru. In: Glascock, M.D., Speakman, R.J., Popelka-Filcoff, R.S. (Eds.), Archaeological Chemistry: Analytical Techniques and Archaeological Interpretation. American Chemical Society, Washington, D.C, pp. 480–505.
Popelka-Filcoff, R.S., Miksa, E.J., Robertson, J.D., Glascock, M.D., Wallace, H., 2008. Elemental analysis and characterization of ochre sources from southern Arizona. Journal of Archaeological Science 35, 752–762.
Posnansky, M., Nelson, C.M., 1968. Rock paintings and excavations at Nyero, Uganda. Azania 3, 147–166.
Randel, R.P., Johnson, R.W., 1991. Geology of the Suswa Area. Report No. 97. Mines and Geological Department, Government of Kenya, Nairobi.
Ren, M., Omenda, P.A., Anthony, E.Y., White, J.C., MacDonald, R., Bailey, D.K., 2006. Application of the QUILF thermobarometer to the peralkaline trachytes and pantellerites of the Eburru volcanic complex, East African Rift, Kenya. Lithos 91, 109–124.
Renfrew, C., Dixon, J.E., Cann, J.R., 1966. Obsidian and early cultural contact in the Near East. Proceedings of the Prehistoric Society (New Series) 32, 30–72.
Rifkin, R., 2011. Assessing the efficacy of red ochre as a prehistoric hide tanning ingredient. Journal of African Archaeology 9, 131–158.
Rifkin, R.F., Dayet, L., Queffelec, A., Summers, B., Lategan, M., d'Errico, F., 2015. Evaluating the photoprotective effects of ochre on human skin by in vivo SPF assessment: implications for human evolution, adaptation and dispersal. PLoS One 10, e0136090. http://dx.doi.org/10.1371/journal.pone.0136090.
Rifkin, R.F., Prinsloo, L.C., Dayet, L., Haaland, M.M., Henshilwood, C.S., Diz, E.L., Moyo, S., Vogelsang, R., Kambombo, F., 2016. Characterising pigments on 30000-year-old portable art from Apollo 11 Cave, Karas Region, southern Namibia. Journal of Archaeological Science: Reports 5, 336–347.
Robertshaw, P.T., Collett, D.P., 1983. The identification of pastoral peoples in the archaeological record: an example from East Africa. World Archaeology 15, 67–78.
Rogers, N.W., Evans, P.J., Blake, S., Scott, S.C., Hawkesworth, C.J., 2004. Rates and timescales of fractional crystallization from ^{238}U-^{230}Th-^{226}Ra disequilibria in trachyte lavas from Longonot volcano, Kenya. Journal of Petrology 45, 1747–1776.
Rollinson, H.R., 1993. Using Geochemical Data: Evaluation, Presentation, Interpretation. Routledge, London and New York.
Ross, J., Davidson, I., 2006. Rock art and ritual: an archaeological analysis of rock art in arid Central Australia. Journal of Archaeological Method and Theory 13, 305–341.
Russell, T., 2013. Through the skin: exploring pastoralist marks and their meanings to understand parts of East African rock art. Journal of Social Archaeology 13, 3–30.
Saitoti, T.O., 1993. Maasai. Abradale Press, New York.
Sauvet, G., Bourrillon, R., Conkey, M., Fritz, C., Gárate-Maidagan, D., Vilá, O.R., Tosello, G., White, R., 2015a. Uranium–thorium dating method and Palaeolithic rock art. Quaternary International. http://dx.doi.org/10.1016/j.quaint.2015.03.053.
Sauvet, G., Bourrillon, R., Conkey, M., Fritz, C., Gárate-Maidagan, D., Vilá, O.R., Tosello, G., White, R., 2015b. Answer to "Comment on Uranium-thorium dating method and Palaeolithic rock art" by Sauvet et al. (2015, in press) by Pons-Branchu E. et al. Quaternary International. http://dx.doi.org/10.1016/j.quaint.2015.10.016.
Scadding, R., Winton, V., Brown, V., 2015. An LA-ICP-MS trace element classification of ochres in the Weld Range environ, Mid West region, Western Australia. Journal of Archaeological Science 54, 300–312.
Scaillet, B., MacDonald, R., 2003. Experimental constraints on the relationships between peralkaline rhyolites of the Kenya Rift Valley. Journal of Petrology 44, 1867–1894.
Schwertmann, U., Cornell, R.M., 1991. Iron Oxides in the Laboratory: Preparation and Characterization. VCH, Weinheim, Germany.
Simiyu, S.M., 2010. Status of geothermal exploration in Kenya and future plans for its development. In: Proceedings, World Geothermal Congress 2010. Bali, Indonesia, pp. 1–11.

Simpson, G.L., Waweru, P., 2012. Becoming Samburu: the ethnogenesis of a pastoral people in nineteenth-century northern Kenya. The Journal of the Middle East and Africa 3, 175–197.
Skilling, I.P., 1993. Incremental caldera collapse of Suswa volcano, Gregory Rift Valley, Kenya. Journal of the Geological Society, London 150, 885–896.
Speer, C.A., 2014. Experimental sourcing of Edwards Plateau chert using LA-ICP-MS. Quaternary International 342, 199–213.
Spink, P.C., 1945. Thermal activity in the eastern Rift Valley. Geographical Journal 105, 197–207.
Spink, P.C., Stevens, J.A., 1946. Notes on the Magadi section of the eastern Rift Valley. Geographical Journal 107, 236–241.
Sun, S.-S., McDonough, W.F., 1989. Chemical and isotopic systematics of oceanic basalts: implications for mantle composition and processes. Geological Society, London, Special Publications 42, 313–345.
Taçon, P.S., 2008. Rainbow colour and power among the Waanyi of northwest Queensland. Cambridge Archaeological Journal 18, 163–176.
Thackeray, A.I., Thackeray, J.F., Beaumont, P.B., 1983. Excavations at the Blinkklipkop Specularite Mine near Postmasburg, Northern Cape. South African Archaeological Bulletin 38, 17–25.
Thomas, P.S., Stuart, B.H., McGowan, N., Guerbois, J.P., Berkahn, M., Daniel, V., 2011. A study of ochres from an Australian aboriginal bark painting using thermal methods. Journal of Thermal Analysis and Calorimetry 104, 507–513.
Torres-Alvarado, I.S., Pandarinath, K., Verma, S.P., Dulski, P., 2007. Mineralogical and geochemical effects due to hydrothermal alteration in the Los Azufres geothermal field, Mexico. Revista Mexicana de Ciencias Geológicas 24, 15–24.
Trauth, M.H., Deino, A.L., Bergner, A.G.N., Strecker, M.R., 2003. East African climate change and orbital forcing during the last 175 kyr BP. Earth and Planetary Science Letters 206, 297–313.
Vahur, S., Teearu, A., Leito, I., 2010. ATR-FT-IR spectroscopy in the region of 550-230 cm^{-1} for identification of inorganic pigments. Spectrochimica Acta A 75, 1061–1072.
Velador, J.M., Omenda, P.A., Anthony, E.Y., 2002. Geology and the origin of trachytes and pantellerites from the Eburru volcanic field, Kenya Rift. In: AGU Fall Meeting Abstracts 2002, p. 1416.
Velador, J., Omenda, P., Anthony, E., 2003. An integrated GIS-remote sensing study of the geology and structural controls of fumarole locations, Eburru volcanic field, Kenya Rift. Geothermal Resources Council Transactions 27, 639–642.
Velo, J., 1984. Ochre as medicine: a suggestion for the interpretation of the archaeological record. Current Anthropology 25, 674.
Wadley, L., Williamson, B., Lombard, M., 2004. Ochre in hafting in Middle Stone Age southern Africa: a practical role. World Archaeology 26, 19–34.
Watts, I., 1999. The origin of symbolic culture. In: Dunbar, R., Knight, C., Power, C. (Eds.), The Evolution of Culture: an Interdisciplinary View. Edinburgh University Press, Edinburgh, pp. 113–146.
Watts, I., 2009. Red ochre, body painting and language: interpreting the Blombos ochre. In: Botha, R., Knight, C. (Eds.), The Cradle of Language. Oxford University Press, Oxford, pp. 62–92.
Watts, I., 2014. The red thread: pigment use and the evolution of collective ritual. In: Dor, D., Knight, C., Lewis, J. (Eds.), The Social Origins of Language. Oxford University Press, Oxford, pp. 208–227.
Weigand, P.C., Harbottle, G., Sayre, E.V., 1977. Turquoise sources and source analysis: Mesoamerican and the Southwestern U.S.A. In: Earle, T.K., Ericson, J.E. (Eds.), Exchange Systems in Prehistory. Academic Press, New York, pp. 15–34.
Weill, D.F., Drake, M.J., 1973. Europium anomaly in plagioclase feldspar: experimental results and semiquantitative model. Science 180, 1059–1060.
Weltje, G.J., von Eynatten, H., 2004. Quantitative provenance analysis of sediments: review and outlook. Sedimentary Geology 171, 1–11.
White, J.C., Espejel-García, V.V., Anthony, E.Y., Omenda, P.A., 2012a. Petrogenesis of the Suswa volcano, Kenya. Proceedings of the 4th African Rift Geothermal Conference. Nairobi, Kenya, pp. 2–14.
White, J.C., Espejel-García, V.V., Anthony, E.Y., Omenda, P.A., 2012b. Open system evolution of peralkaline trachyte and phonolite from the Suswa volcano, Kenya Rift. Lithos 152, 84–104.
Wilson, L., Pollard, A.M., 2001. The provenance hypothesis. In: Brothwell, D.R., Pollard, A.M. (Eds.), Handbook of Archaeological Sciences. John Wiley and Sons, Ltd., Chichester, pp. 507–517.
Wooley, A.R., 2001. Alkaline Rocks and Carbonatites of the World: Africa. The Geological Society of London, Bath.
Wreschner, E.E., Bolton, R., Butzer, K.W., Delporte, H., Häusler, A., Heinrich, A., Jacobson-Widding, A., Malinowski, T., Masset, C., Miller, S.F., Ronen, A., Solecki, R., Stephenson, P.H., Thomas, L.L., Zollinger, H., 1980. Red Ochre and human evolution: a case for discussion [and comments and reply]. Current Anthropology 21, 631–644.
Wynn, T., Tierson, F., 1990. Regional comparison of the shapes of later Acheulean handaxes. American Anthropologist 92, 73–84.
Yokoyama, T., Nakashima, S., 2005. Color development of iron oxides during rhyolite weathering over 52,000 years. Chemical Geology 219, 309–320.
Zipkin, A.M., Hanchar, J.M., Brooks, A.S., Grabowski, M.W., Thompson, J.C., Gomani-Chindebvu, E., 2015. Ochre fingerprints: distinguishing among Malawian mineral pigment sources with homogenized ochre chip LA-ICPMS. Archaeometry 57, 297–317.
Zipkin, A.M., Wagner, M., McGrath, K., Brooks, A.S., Lucas, P.W., 2014. An experimental study of hafting adhesives and the implications for compound tool technology. PLoS One 9, e112560. http://dx.doi.org/10.1371/journal.pone.0112560.